



DEPFET Pixel Detector for Belle II

Hua Ye (DESY)

(hua.ye@desy.de)

2019.09, IHEP, Beijing

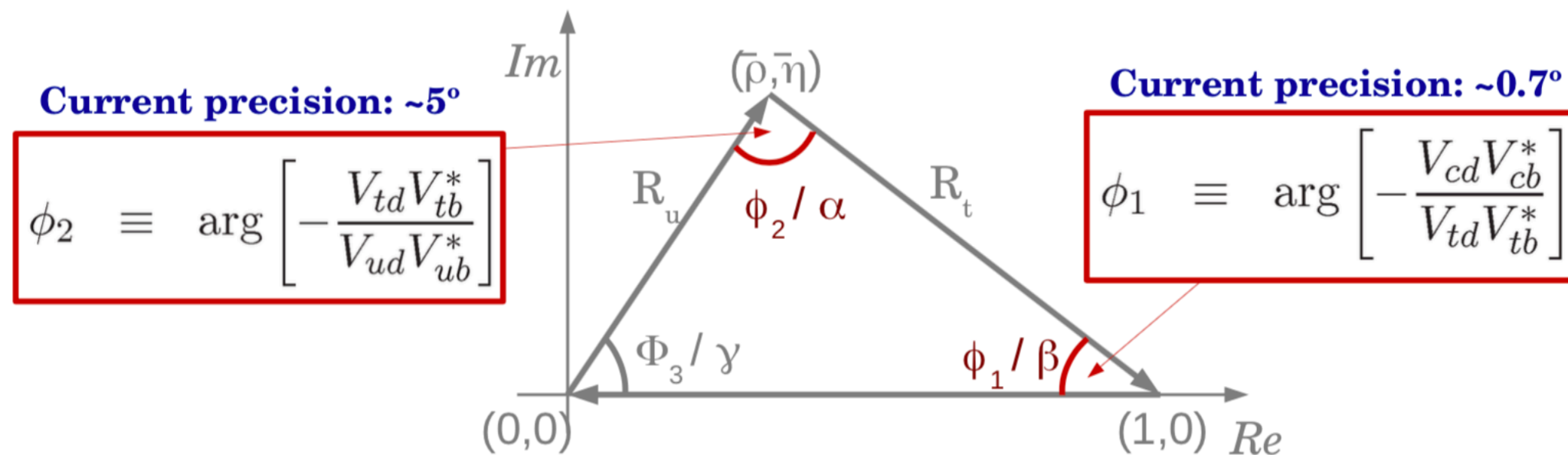
CP Violation and CKM Matrix

❖ The strength of the coupling of quarks via the charged weak current is described by the Cabibbo-Kobayashi-Maskawa (CKM) Matrix.

$$V_{CKM} = \begin{pmatrix} V_{ud} & V_{us} & V_{ub} \\ V_{cd} & V_{cs} & V_{cb} \\ V_{td} & V_{ts} & V_{tb} \end{pmatrix}$$

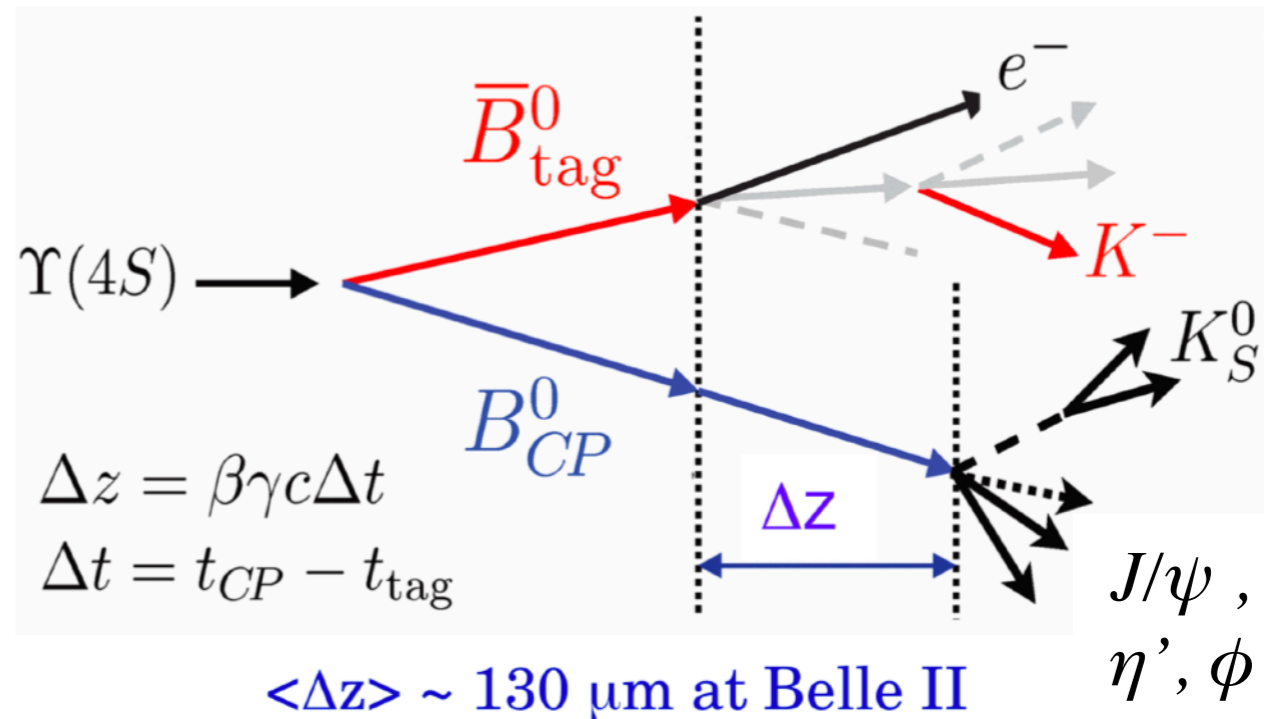
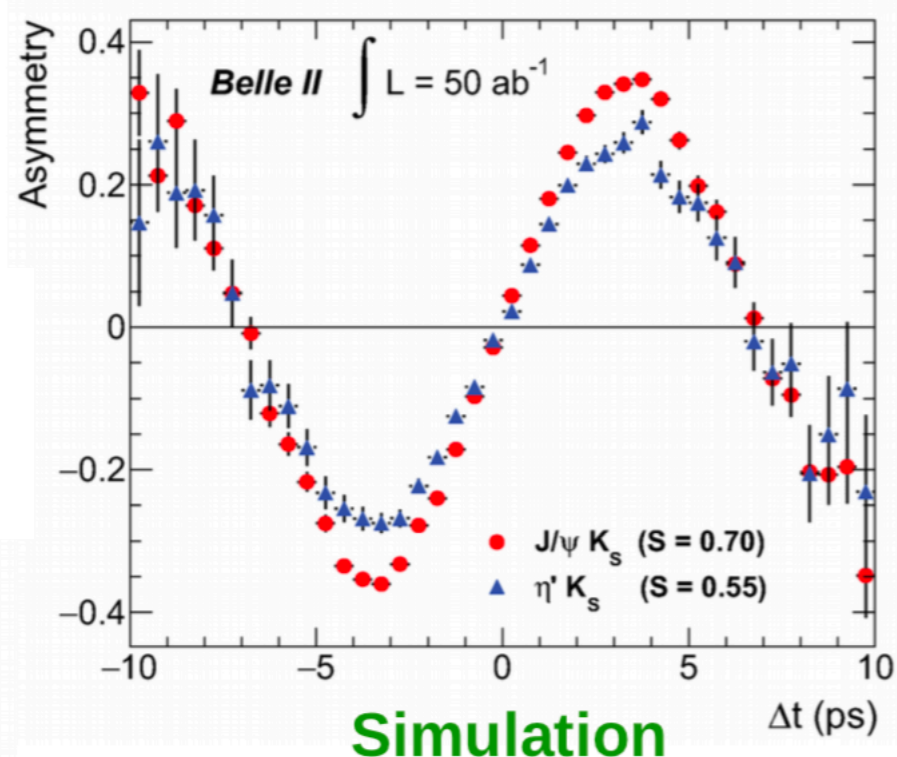
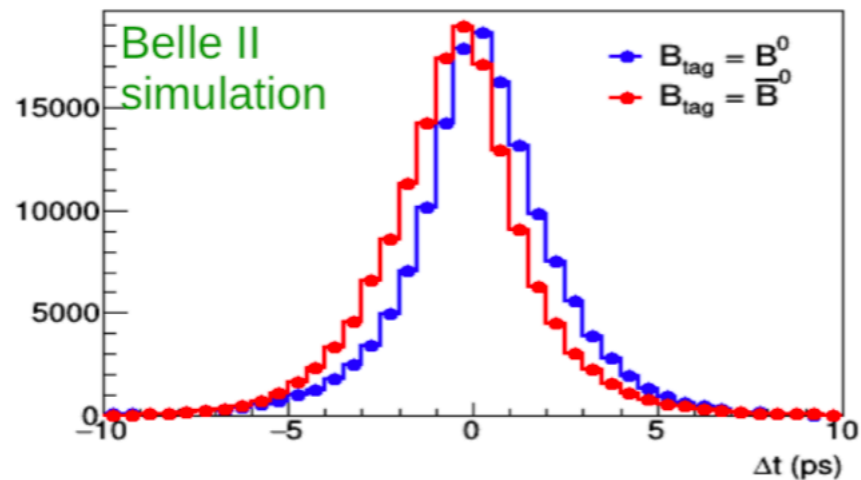
❖ Its unitarity constraints define the CKM Unitarity Triangles.

$$V_{ud} V_{ub}^* + V_{cd} V_{cb}^* + V_{td} V_{tb}^* = 0$$



❖ Time dependent CP violation measurements in B_d decays allow us to measure the angles ϕ_1 and ϕ_2 .

Time Dependent CP Violation Measurements



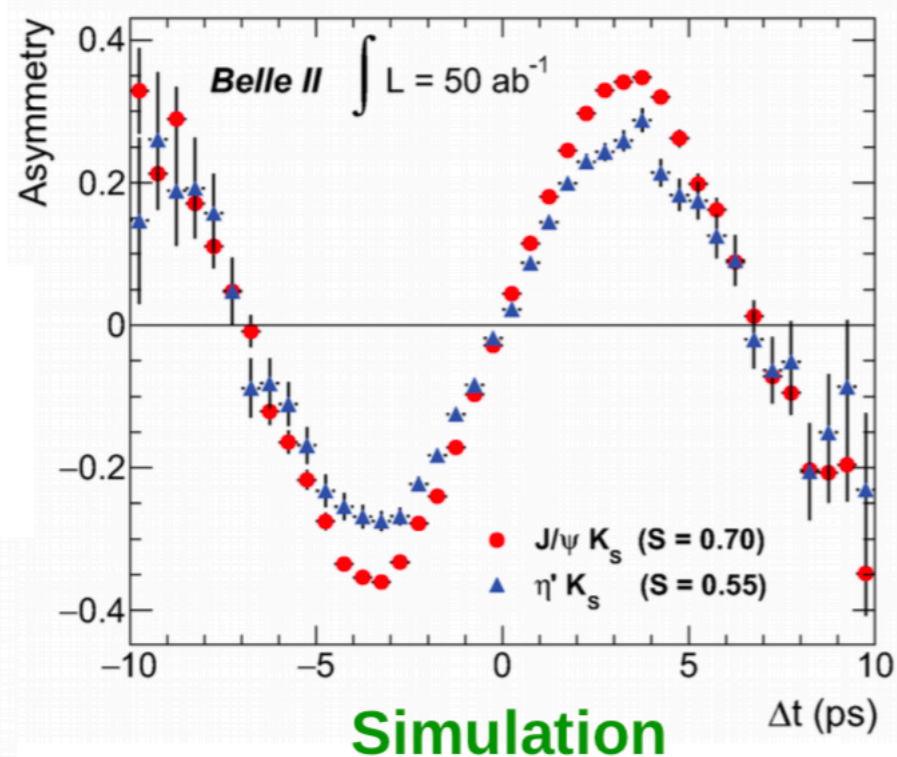
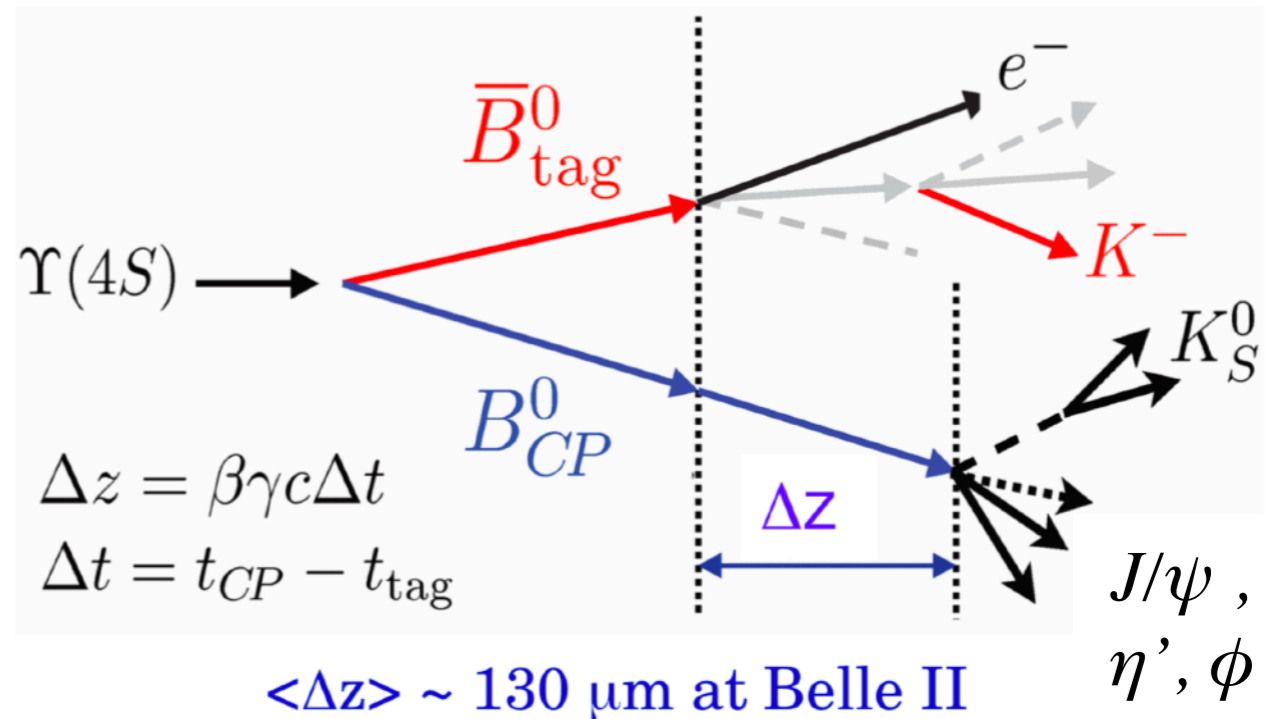
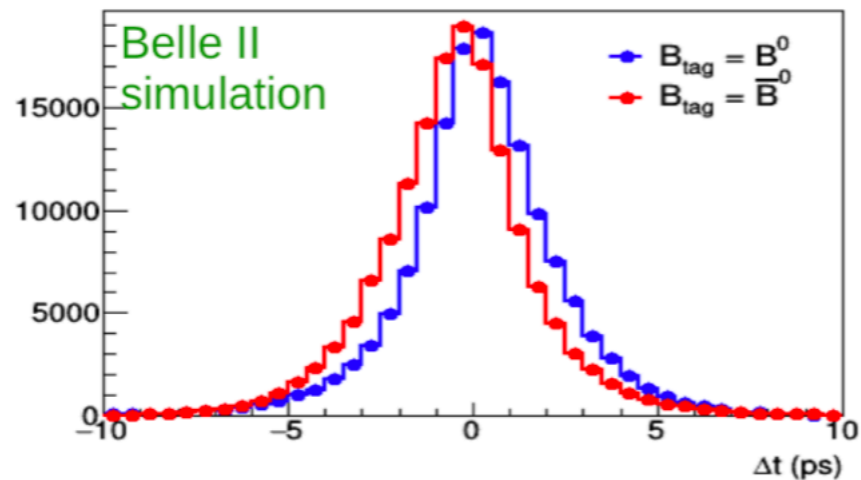
$$\mathcal{A}_f(\Delta t) = \frac{\Gamma(\bar{B}^0(\Delta t) \rightarrow \eta' K_S^0) - \Gamma(B^0(\Delta t) \rightarrow \eta' K_S^0)}{\Gamma(\bar{B}^0(\Delta t) \rightarrow \eta' K_S^0) + \Gamma(B^0(\Delta t) \rightarrow \eta' K_S^0)}$$

$$= S_f \sin(\Delta m_B \Delta t) + A_f \cos(\Delta m_B \Delta t)$$

$$S_f = -\eta_f \sin 2\phi_1$$

- ❖ Tree-dominated $b \rightarrow c\bar{c}s$, golden mode $B^0 \rightarrow J/\psi K_S$, theoretically and experimentally precise.
- ❖ Gluonic-penguin-dominated $b \rightarrow q\bar{q}s$, e.g. $B^0 \rightarrow \phi K_S, \eta' K_S$, particularly sensitive to new physics.
- ❖ Statistical error is still dominated in the measurements of angles of the unitarity triangle.

Time Dependent CP Violation Measurements



- ❖ Tree-dominated $b \rightarrow c\bar{c}s$, golden mode $B^0 \rightarrow J/\psi K_S$
- ❖ Gluonic-penguin-dominated $b \rightarrow q\bar{q}s$, e.g. $B^0 \rightarrow \phi K_S, \eta' K_S$, particularly sensitive to new physics.
- ❖ Statistical error is still dominated in the measurements of angles of the unitarity triangle.

Belle II Experiment

Flavour Physics @Belle II

- ❖ Precise measurements of CKM matrix elements and their phases.
- ❖ Are there new sources of CP violation in the quark sector?
 - ❖ time-dependent CP violation in penguin transitions $b \rightarrow qqs$ quarks, such as $B \rightarrow \phi K^0$ and $B \rightarrow \eta' K^0$
- ❖ Multiple Higgs bosons?
 - ❖ Search charged Higgs in flavour transitions to τ leptons, including $B \rightarrow \tau \nu$ and $B \rightarrow D^{(*)} \tau \nu$.
- ❖ Flavour-changing neutral currents beyond the SM?
 - ❖ forward-backward asymmetries of $b \rightarrow s l^+ l^-$
- ❖ Lepton flavour violation (LFV)

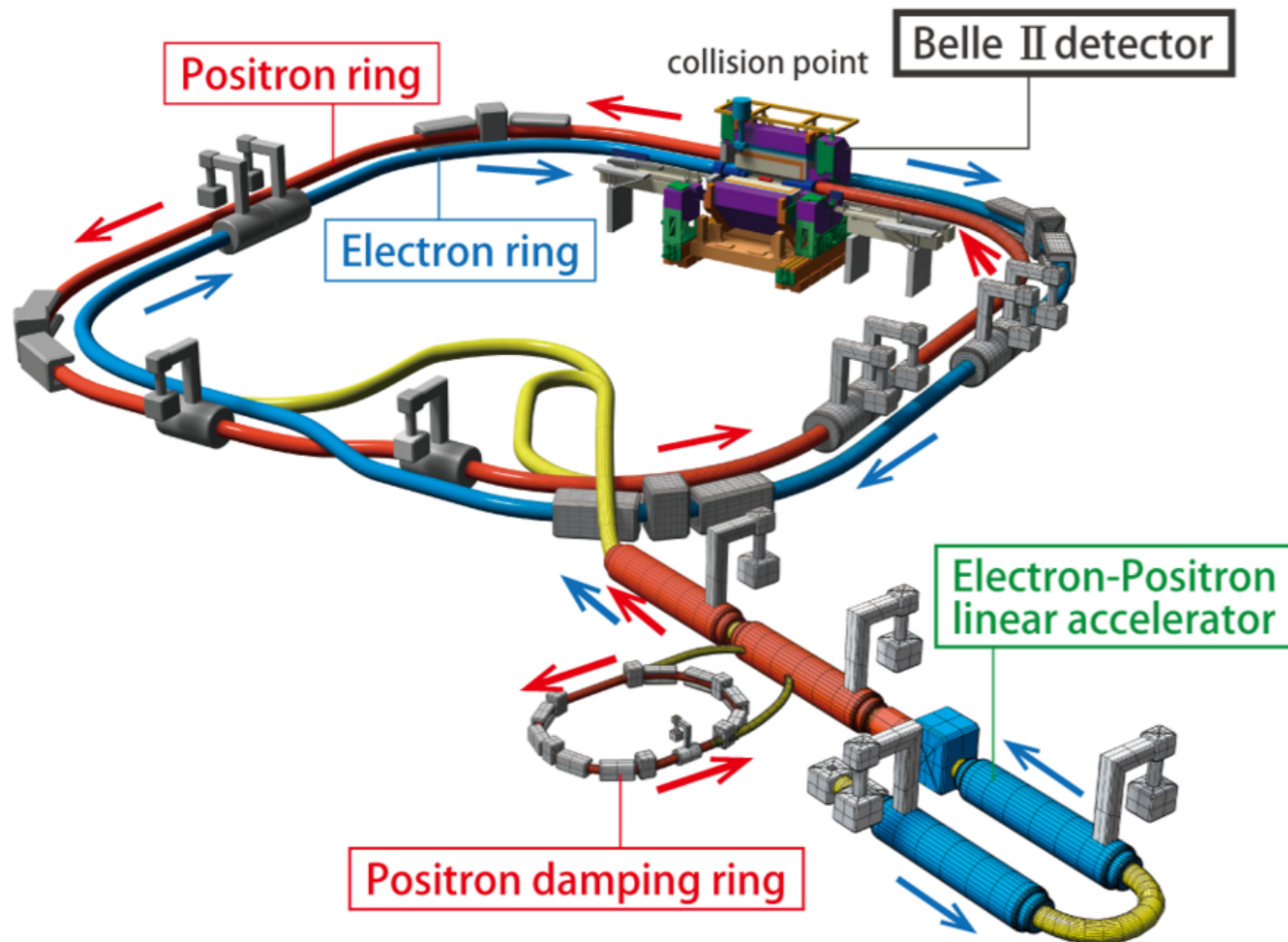
Non-Flavour Physics @Belle II

- ❖ States not predicted by the conventional hadron interpretation.
- ❖ Dark sector

SuperKEKB



Design peaking luminosity is $8 \times 10^{35} \text{ cm}^{-2}\text{s}^{-1}$

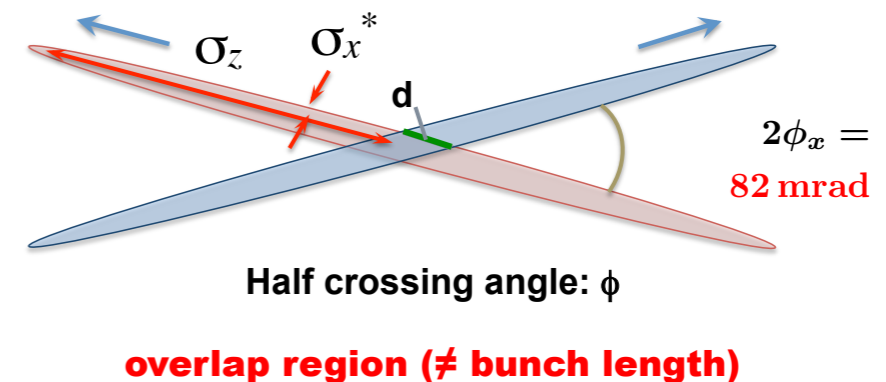


$$L = \frac{\gamma_{\pm}}{2er_e} (1 + a) \frac{R_L}{R_{\xi}} \left(\frac{I_{\pm} \xi_{y\pm}}{\beta_{y\pm}^*} \right)$$

beam current **x2**
beam-beam param. **x1**
vertical beta function **x20**

Nano-Beam scheme:

Squeeze vertical beta function at the IP (β_{y^*}) and minimize longitudinal size of overlap region.



Strong focusing of beams down to vertical size of $\sim 50\text{nm}$ requires **low emittance beams**, very **sophisticated final focus quadrupoles (QCS)** and a **large crossing angle**.

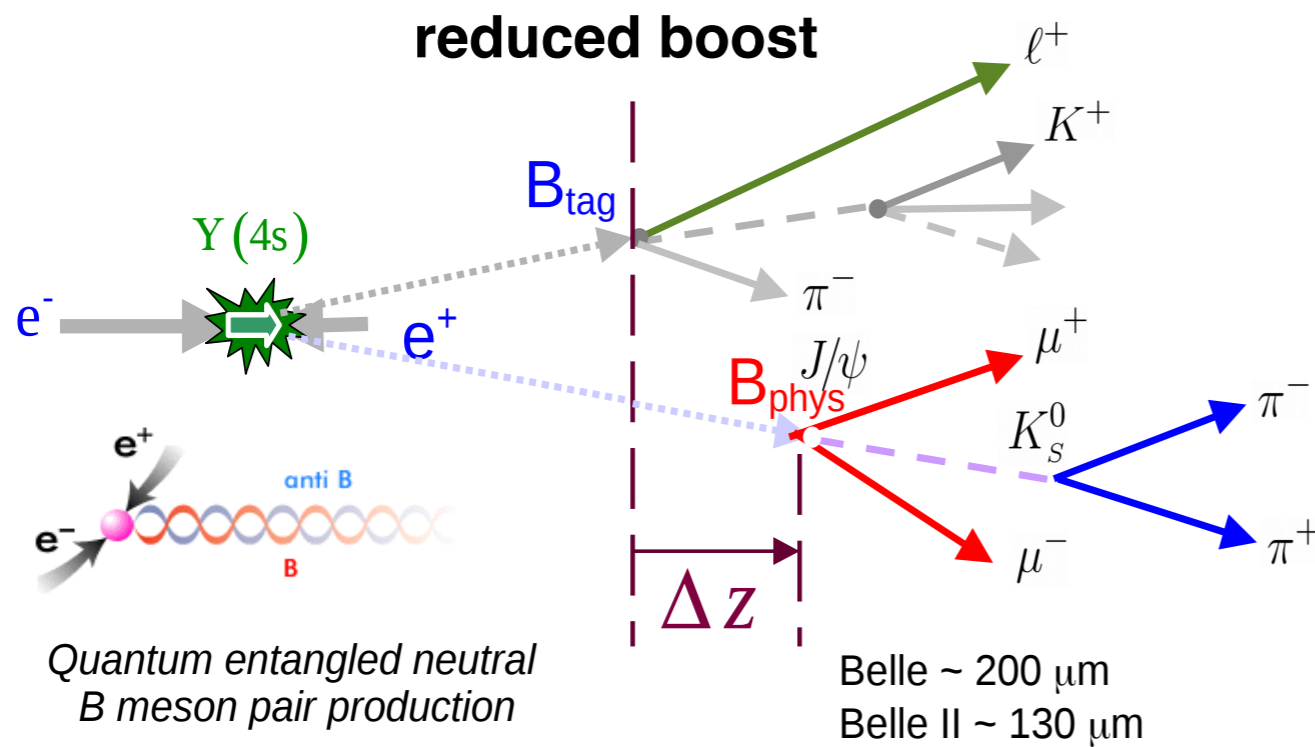
❖ The ultra-high luminosity also increases the background level and trigger rate.

SuperKEKB

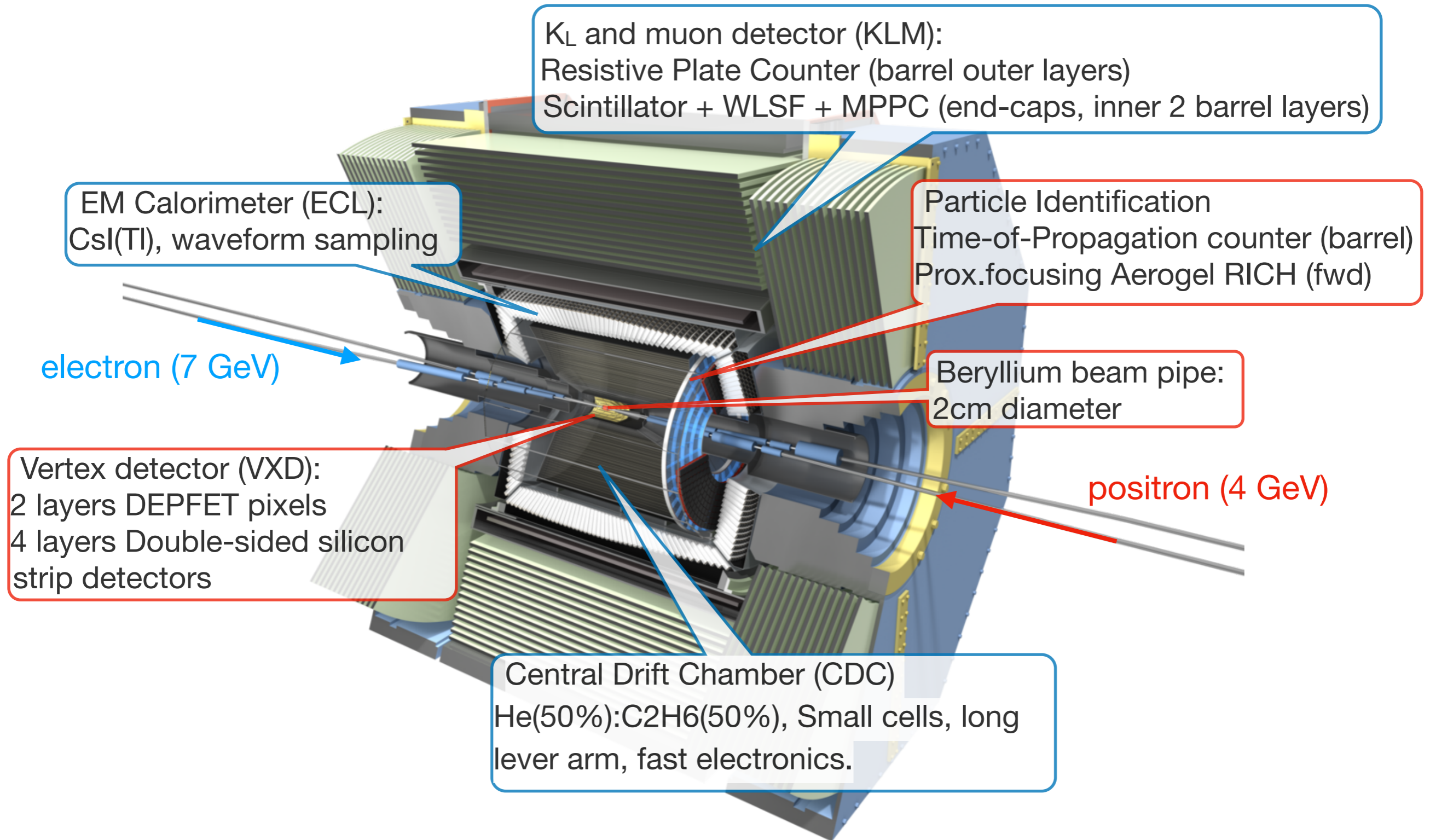


Design peaking luminosity is $8 \times 10^{35} \text{ cm}^{-2}\text{s}^{-1}$

Accelerator	KEKB		SuperKEKB
Beam Energy (GeV)	3.5×8 ($\gamma = 0.425$)		4×7 ($\gamma = 0.28$)
CM energy, $\Upsilon(4S)$,, $\Upsilon(4S)$,
Luminosity ($\text{cm}^{-2}\text{s}^{-1}$)	2.1×10^{34}	$\xrightarrow{\times 40}$	8×10^{35}
Total data (ab^{-1})	1	$\xrightarrow{\times 50}$	50



Belle II Detector



Highlights of Detector Upgrade

- Smaller beam pipe radius allows to place the innermost PXD layer closer to the Interaction point ($r = 1.4 \text{ cm}$)
 - significantly improved vertex resolution
- VXD comprises the PXD of the ultra-low mass DEPFET pixels and larger SVD.
- PID: TOP and ARICH
 - better K/π separation covering the whole momentum range
 - fake rate reduced by factor 2-5
- ECL and KLM consolidation
 - improvements in ECL and KLM to compensate for larger background
- Improved hermeticity
 - geometry and reduced boost
- Improved trigger and DAQ
 - 30 kHz L1 rate
 - 10 kHz HLT output rate (300 kB/evt)

Belle II Vertex Detector

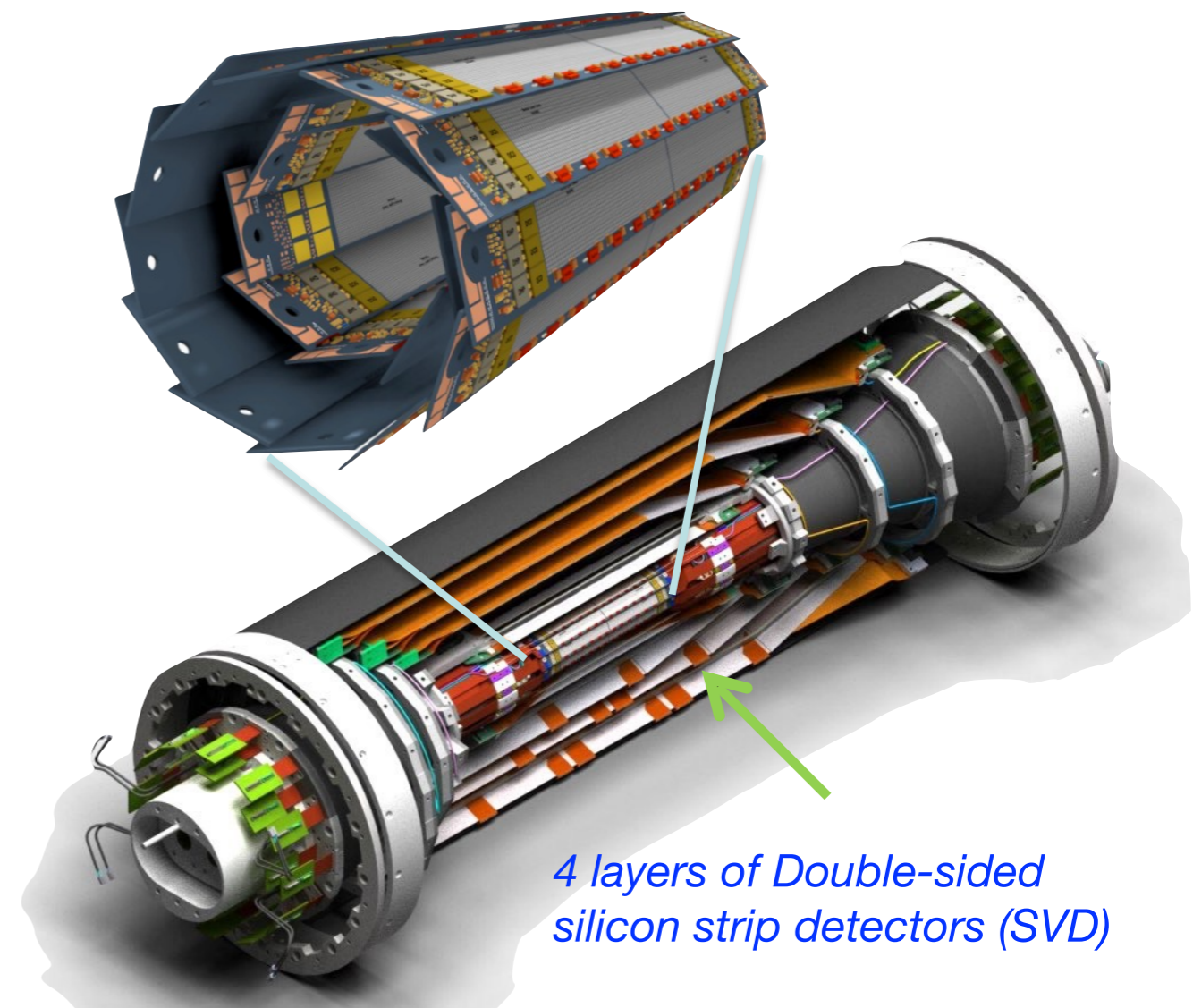
Pixel Detector (PXD)

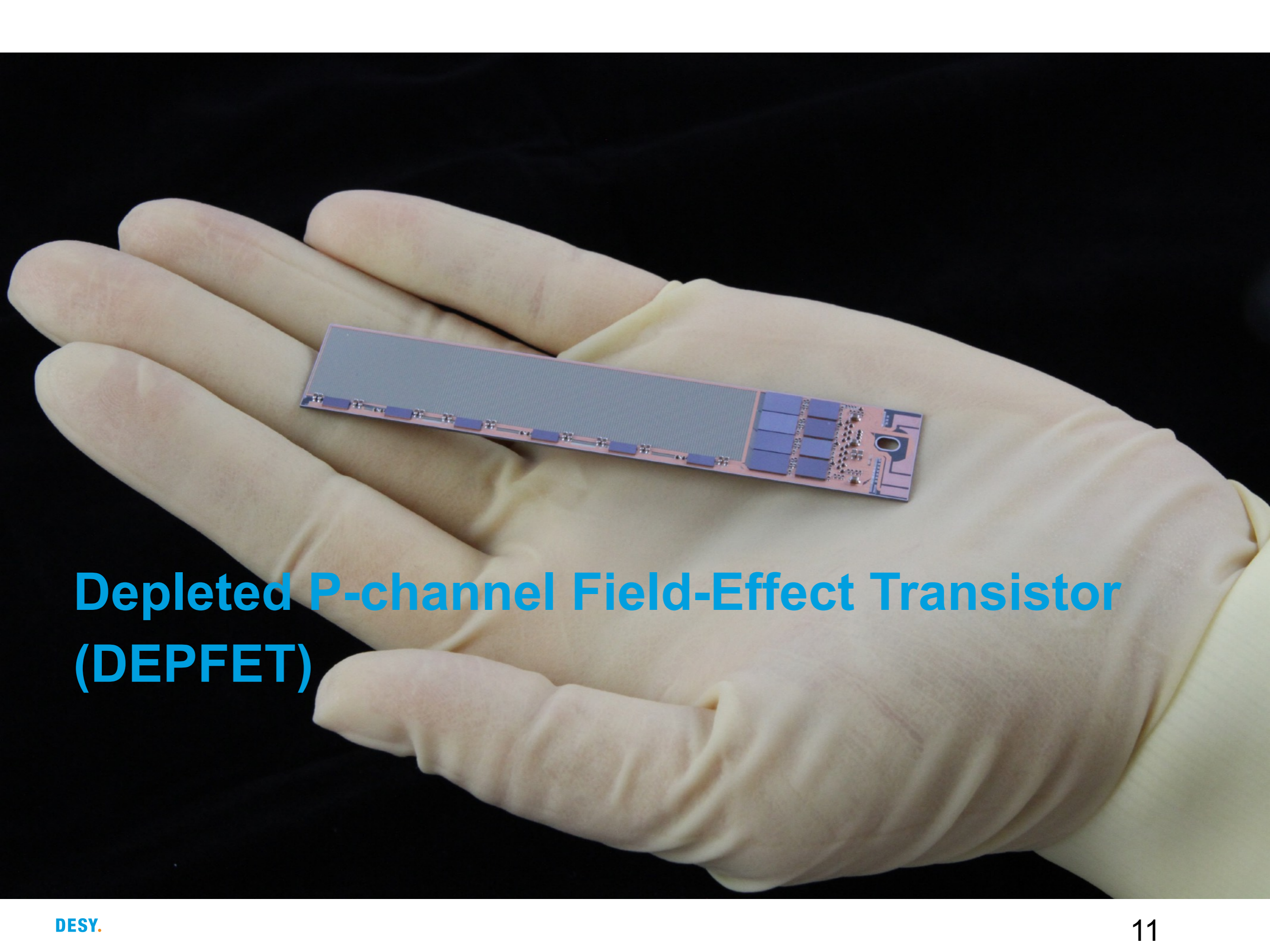
- 2 layers of 40 DEPFET modules @ $r=14/22$ mm
- 250 x 768 pixels per module
- Pixel size: 50 x 55-85 μm^2
- Occupancy: 0.4 hits/ $\mu\text{m}^2/\text{s}$ (3% max)
- Integration time: 20 μs (rolling shutter)
- Thickness: 75 μm , 0.21% X_0 per layer

Silicon Vertex Detector(SVD)

- 4 layers of 172 double-sided silicon strip detectors (DSSDs) @ $r=3.8/8.0/11.5/14\text{cm}$;
- 768 strips in p-side, 768(512)strips in n-side.
- Slant shapes in FWD region for the material budget reduction.
- material budget: 0.7% X_0 per layer

2 layers of DEPFET pixel detector (PXD)

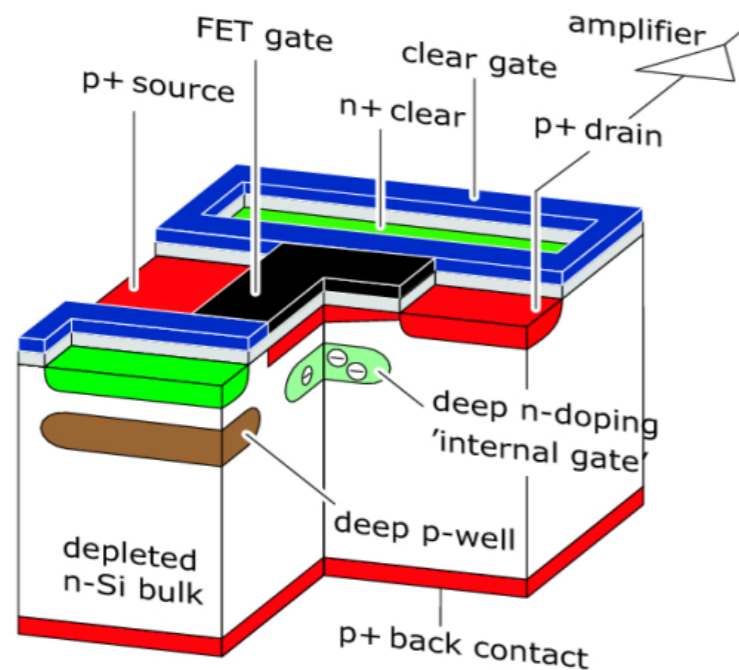




Depleted P-channel Field-Effect Transistor (DEPFET)

DEPFET Pixels

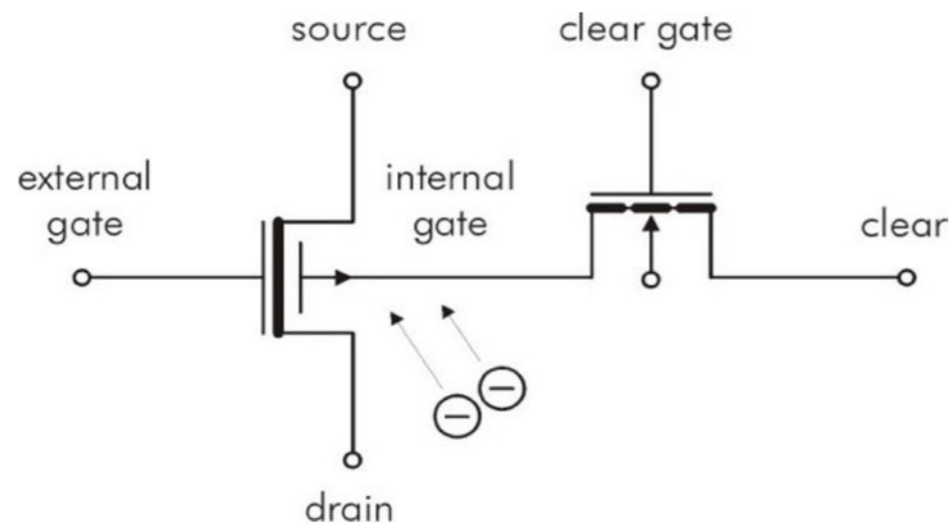
DEPFET provides radiation detection, fast charge collection and internal amplification.



Each pixel is a p-channel FET on top of fully depleted silicon bulk

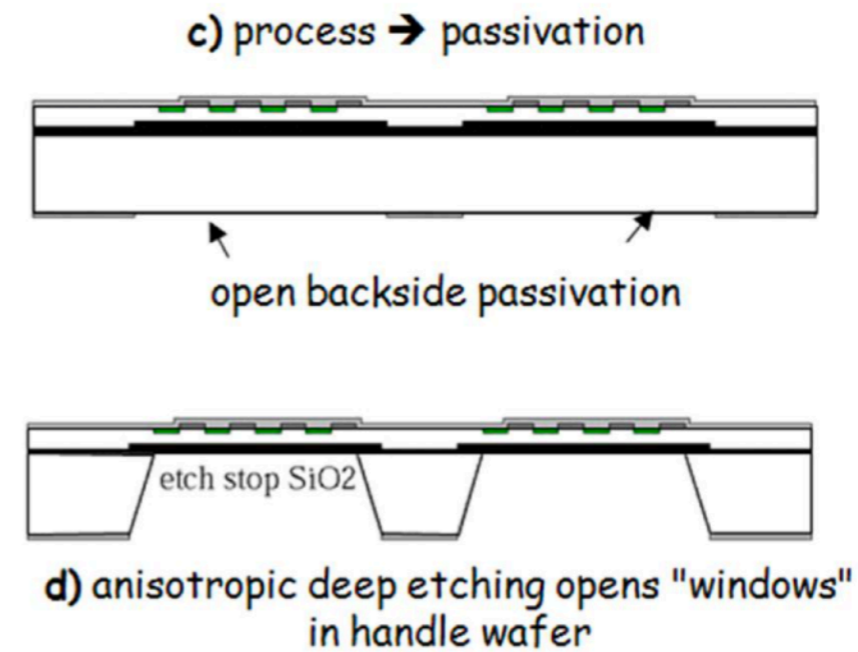
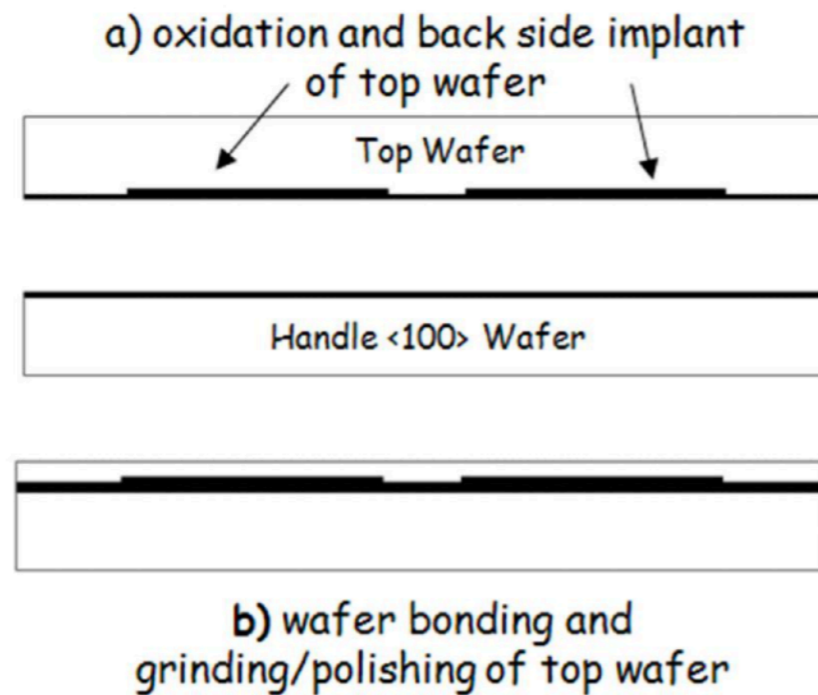
- ❖ Fast charge collection (~ns)
- ❖ Charges collected in the “internal gate”
- ❖ Readout of modulated drain current
 - ➔ internal amplification

$$g_q = \frac{\partial I}{\partial q} \approx 500 \frac{pA}{e^-}$$

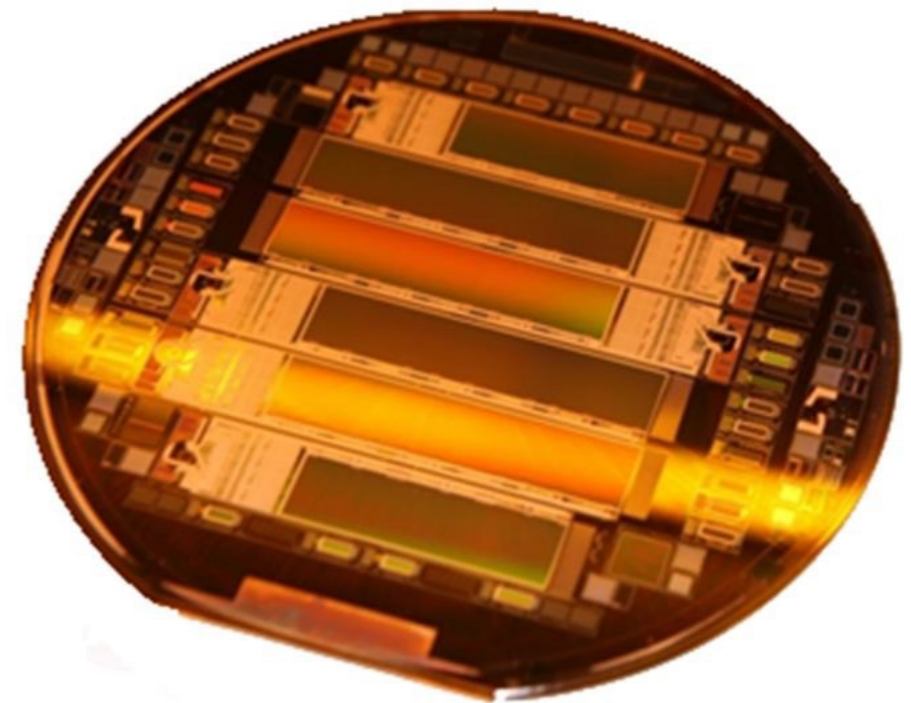


- ❖ High Signal to Noise Ratio (SNR)
- ❖ Periodical clearing of “internal gate” required to reset the pixel

Module Production

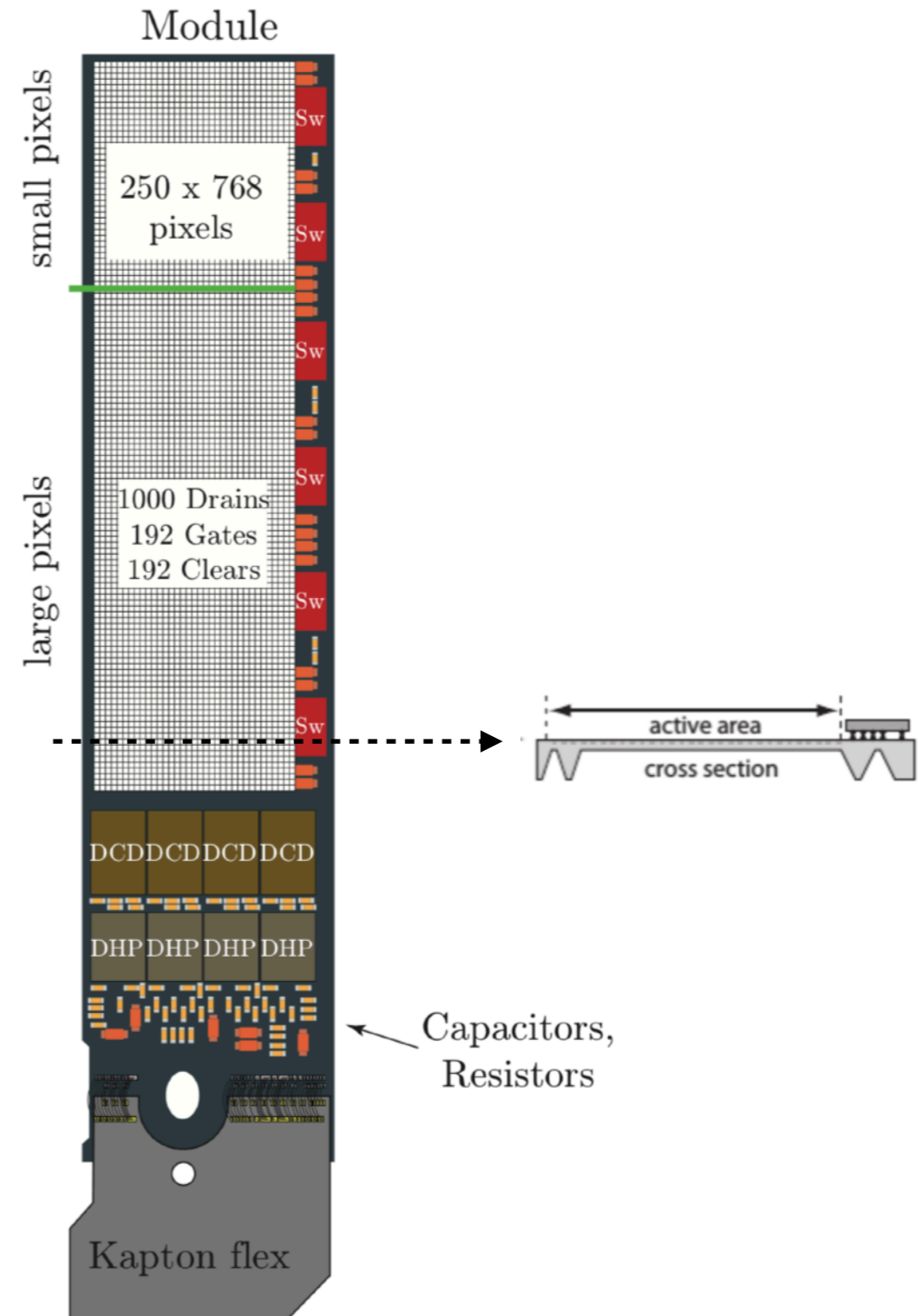


- ❖ Highly granulated pixel detector with ultra-low mass (down to 50 μ m)
- ❖ Key Process Modules:
 - Wafer bonding and thinning of the top layer
 - Sensor fabrication on SOI
 - Etching of the handle wafer



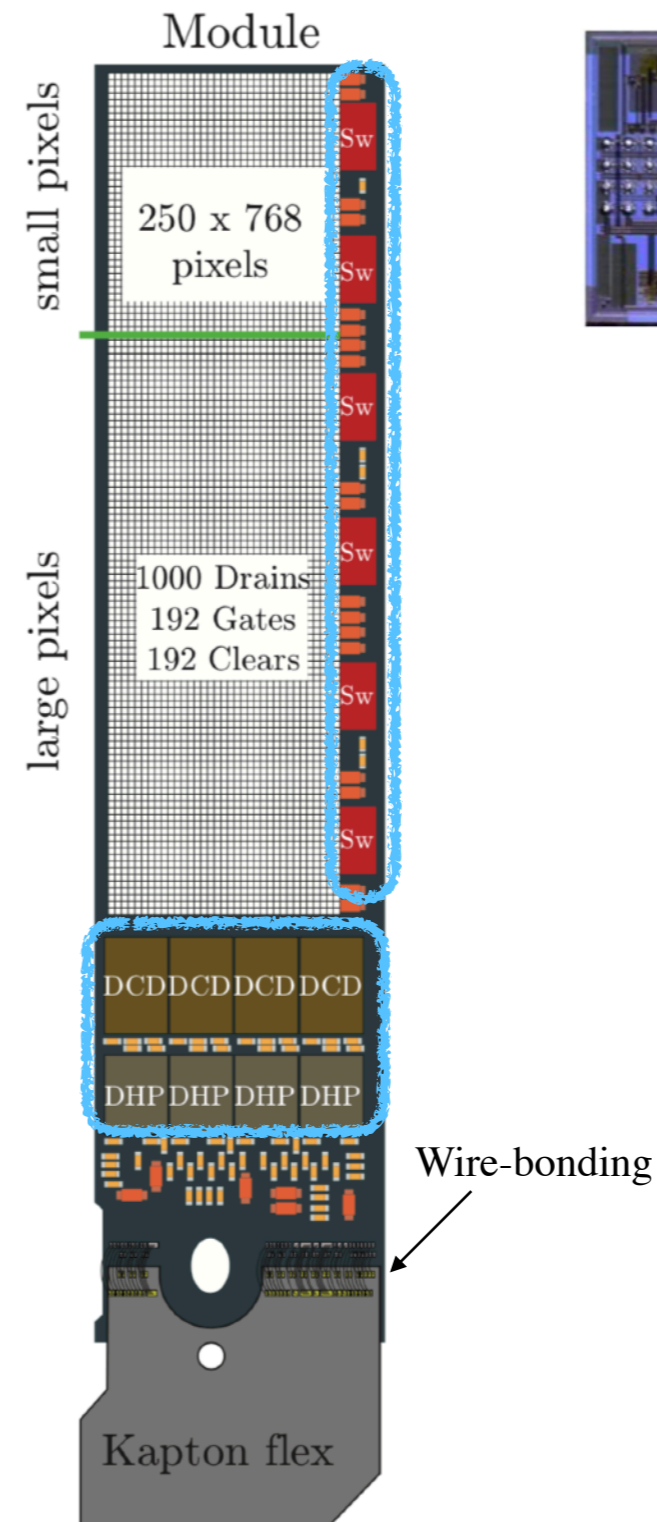
PXD Module Concept

- ❖ Pixel size: varies in z direction, $50 \times 55\text{-}85 \mu\text{m}^2$
 - ❖ optimized to have the best resolution in forward direction around 45° incident angle
- ❖ 250×768 pixels per module
- ❖ By thinning the active sensor thickness can be reduced to as little as $50 \mu\text{m}$.
- ❖ For optimal position resolution (COG) $75\mu\text{m}$ were chosen for PXD
- ❖ 3 Metal layers for circuitry
 - ❖ $2\text{Al} + 1\text{Cu}$
- ❖ Mechanically self-supporting device

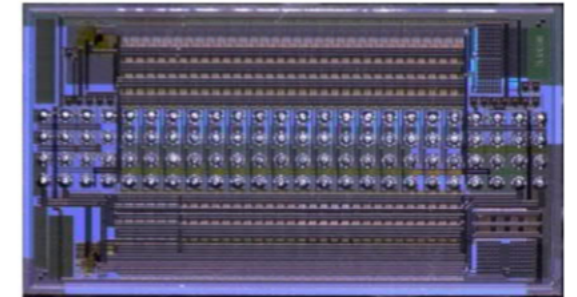


ASICs

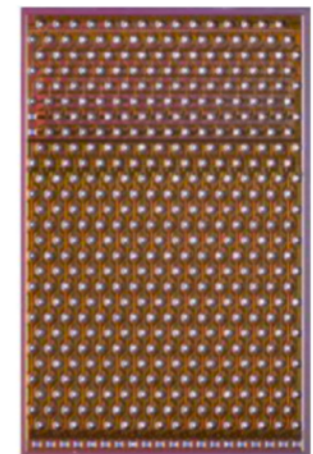
- ❖ 3 types of ASICs are bump-bonded to the module
 - ❖ Switcher: controls the gate and clear lines of the matrix.
 - ❖ DCD: consists of 256 current mode pipeline 8-bit ADCs digitalize the inputs for drain lines.
 - ❖ DHP: digital processor chips, 0-suppression & triggered readout; able to transmit 1.6 Gbit/s of data over a 15 m cable to the backend.



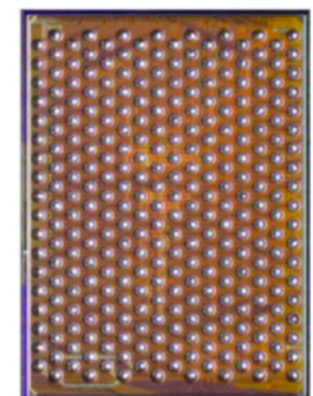
Switcher



DCD

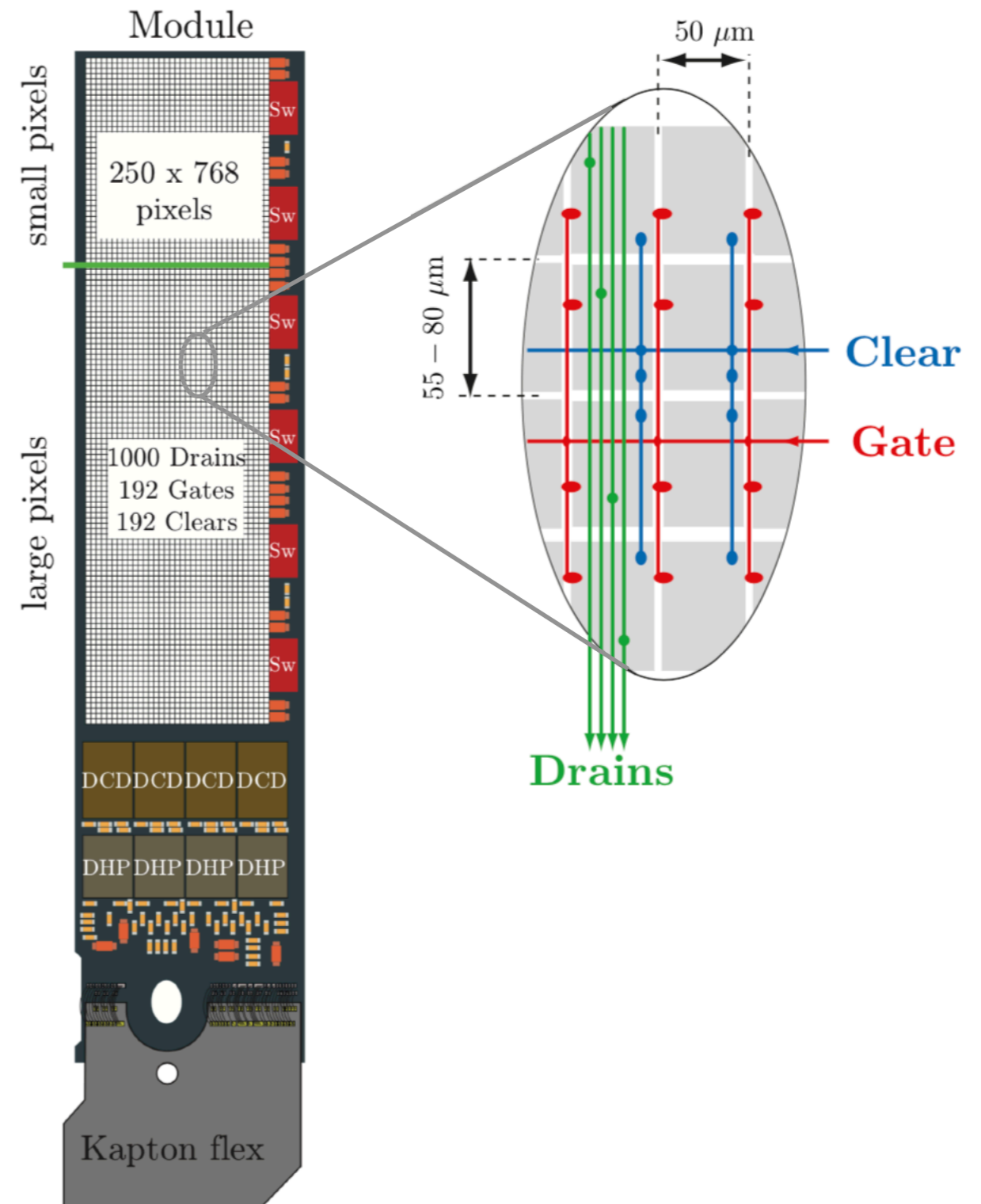


DHP



Readout Mode

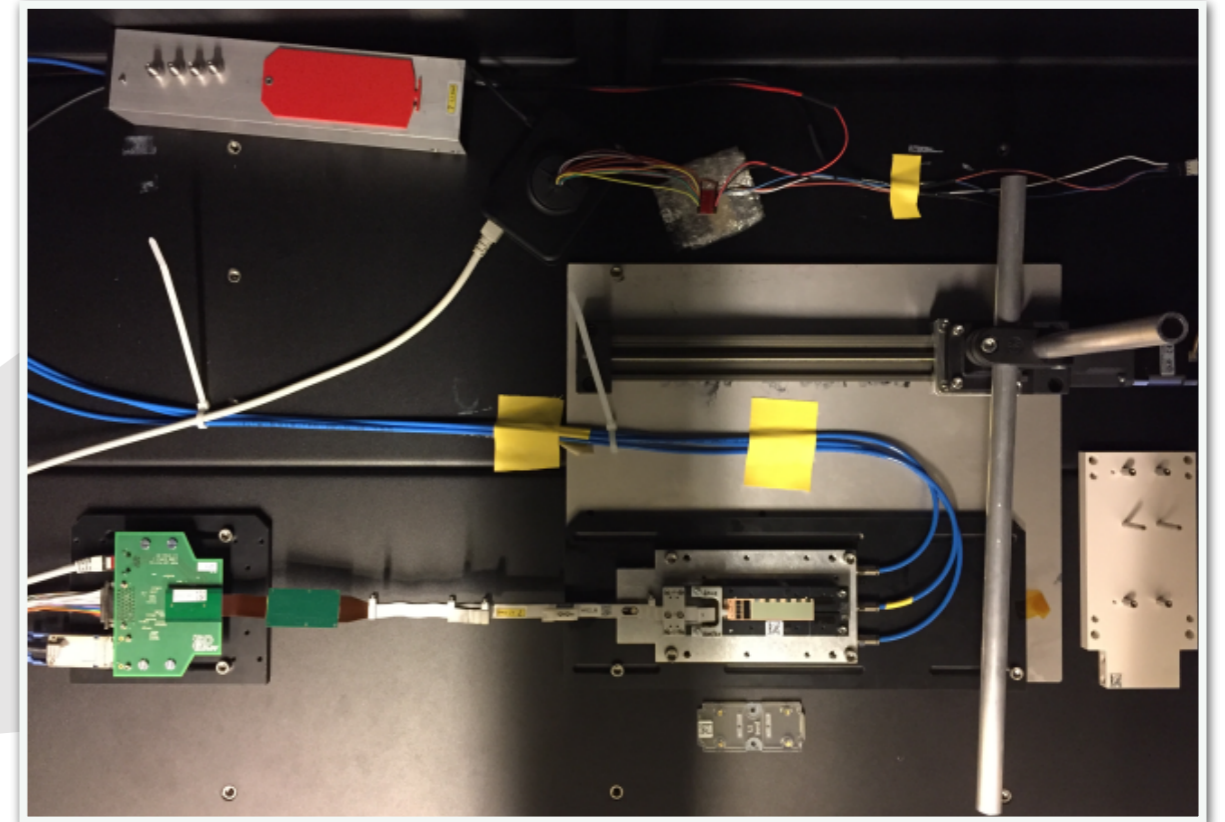
- ❖ Rolling shutter mode
 - ❖ Read signals row-by-row
 - ❖ 4 rows in parallel
 - ❖ Read-Clear cycle in $\sim 100\text{ns}$
 - ❖ Full integration time is $20\mu\text{s}$ (twice the revolution time of SuperKEKB)
 - ❖ Only 'activated' rows consume power
 - ❖ Low sensor power consumption
- ❖ Max. Acceptable average occupancy $< 3\%$, otherwise,
 - ❖ data loss,
 - ❖ degrade tracking performance.



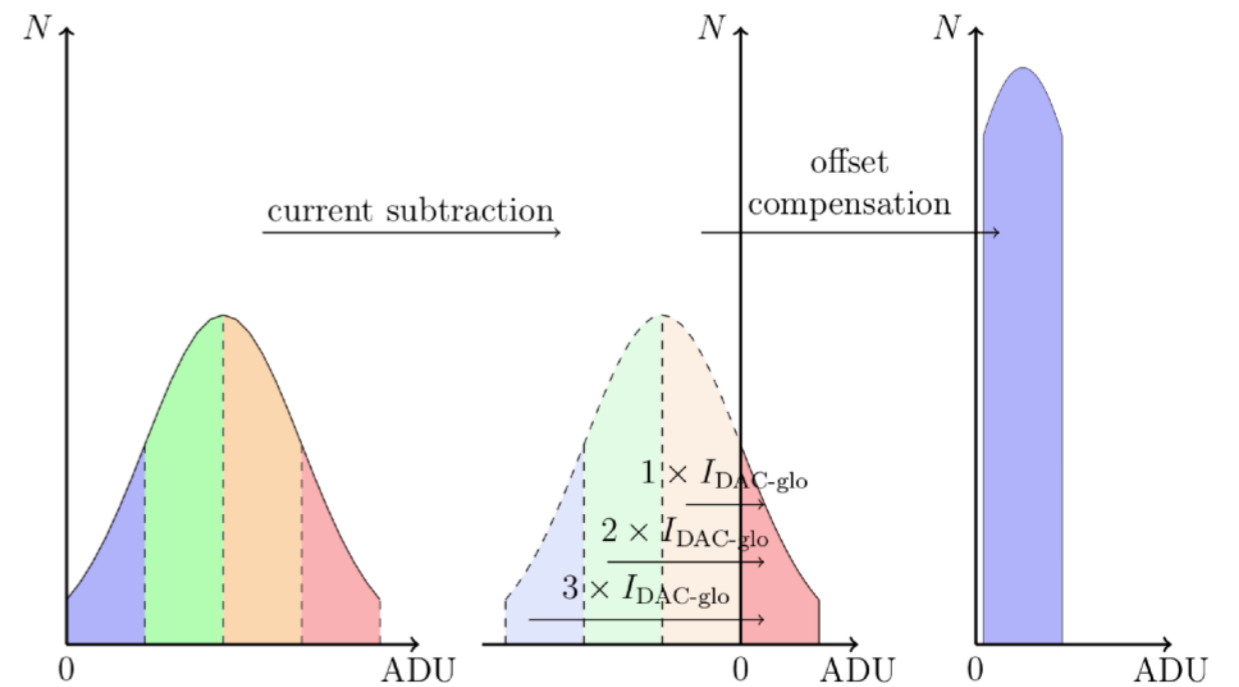
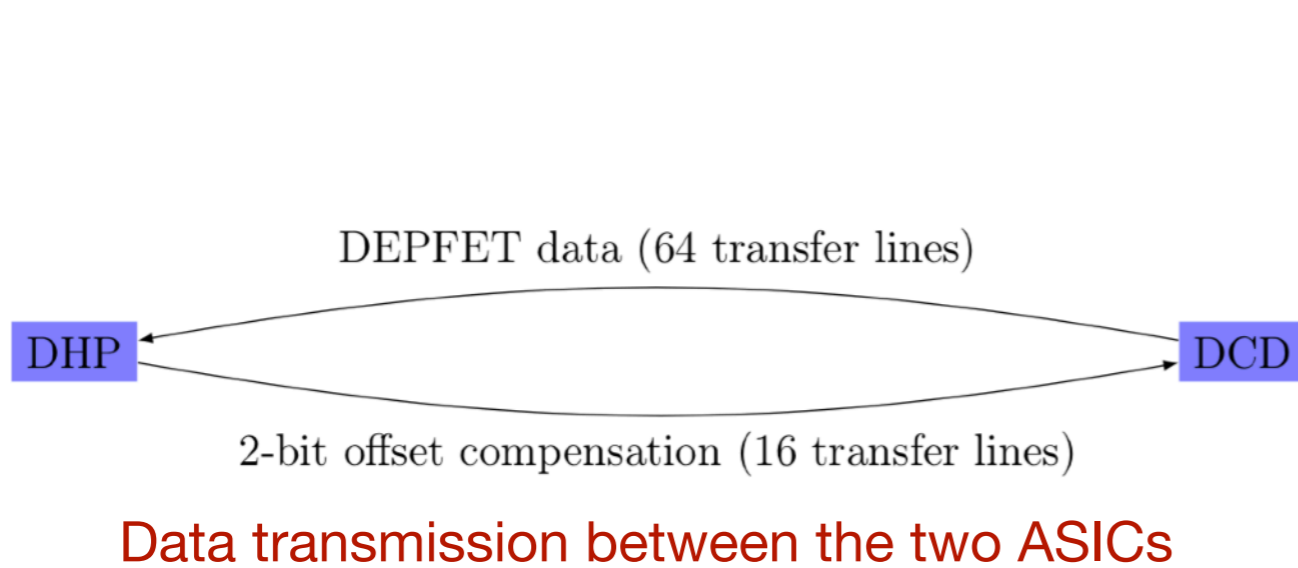
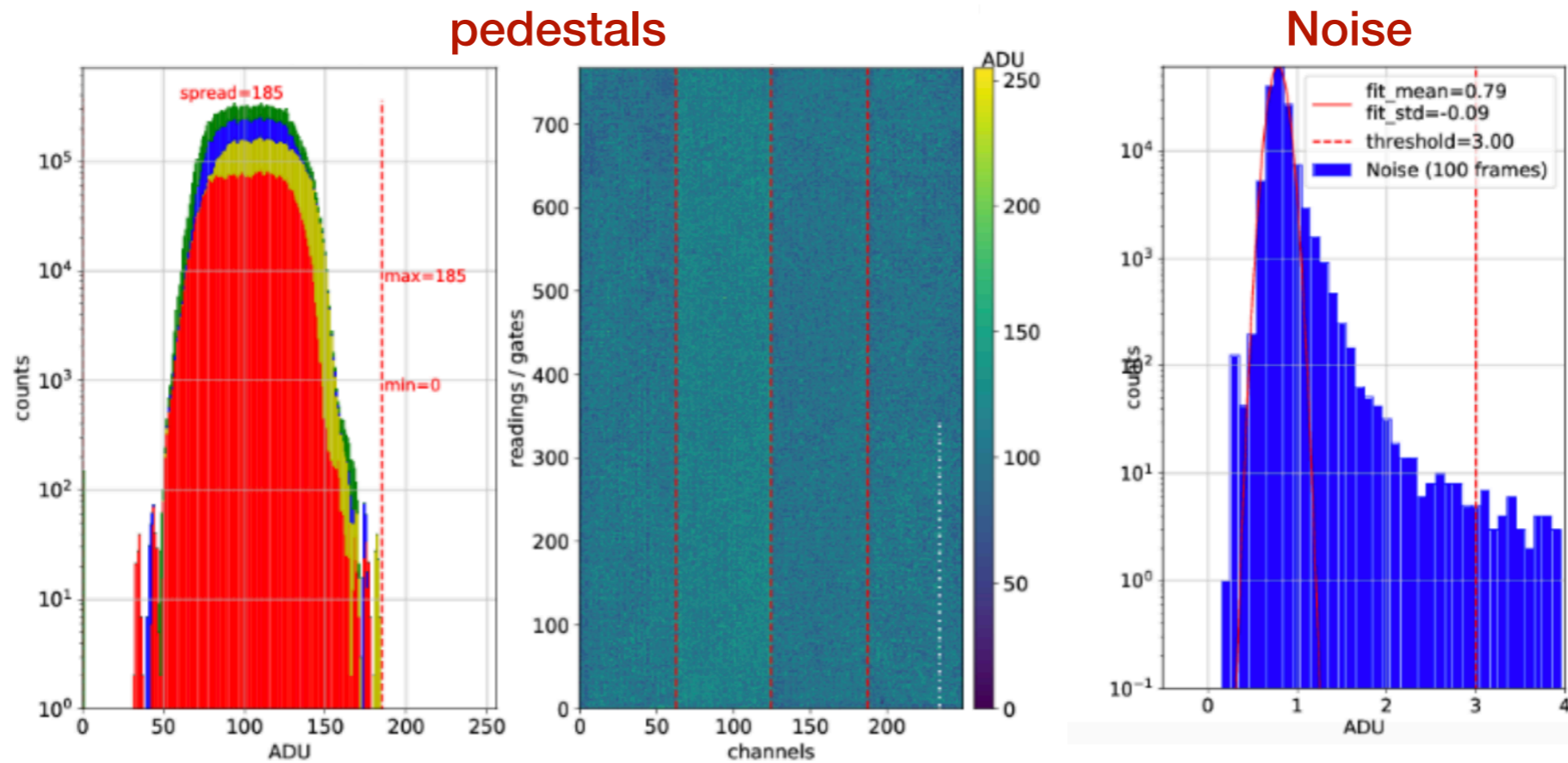
Module Testing

Characterization:

- ❖ High-speed links scan
 - ❖ Find the optimal parameters for stable data transfer
- ❖ Delay scan
 - ❖ Communication between ASICs.
- ❖ Offset calibration
- ❖ ADC curve scan
- ❖ Source scan
 - ❖ To achieve homogeneous response in matrix
- ❖ ...



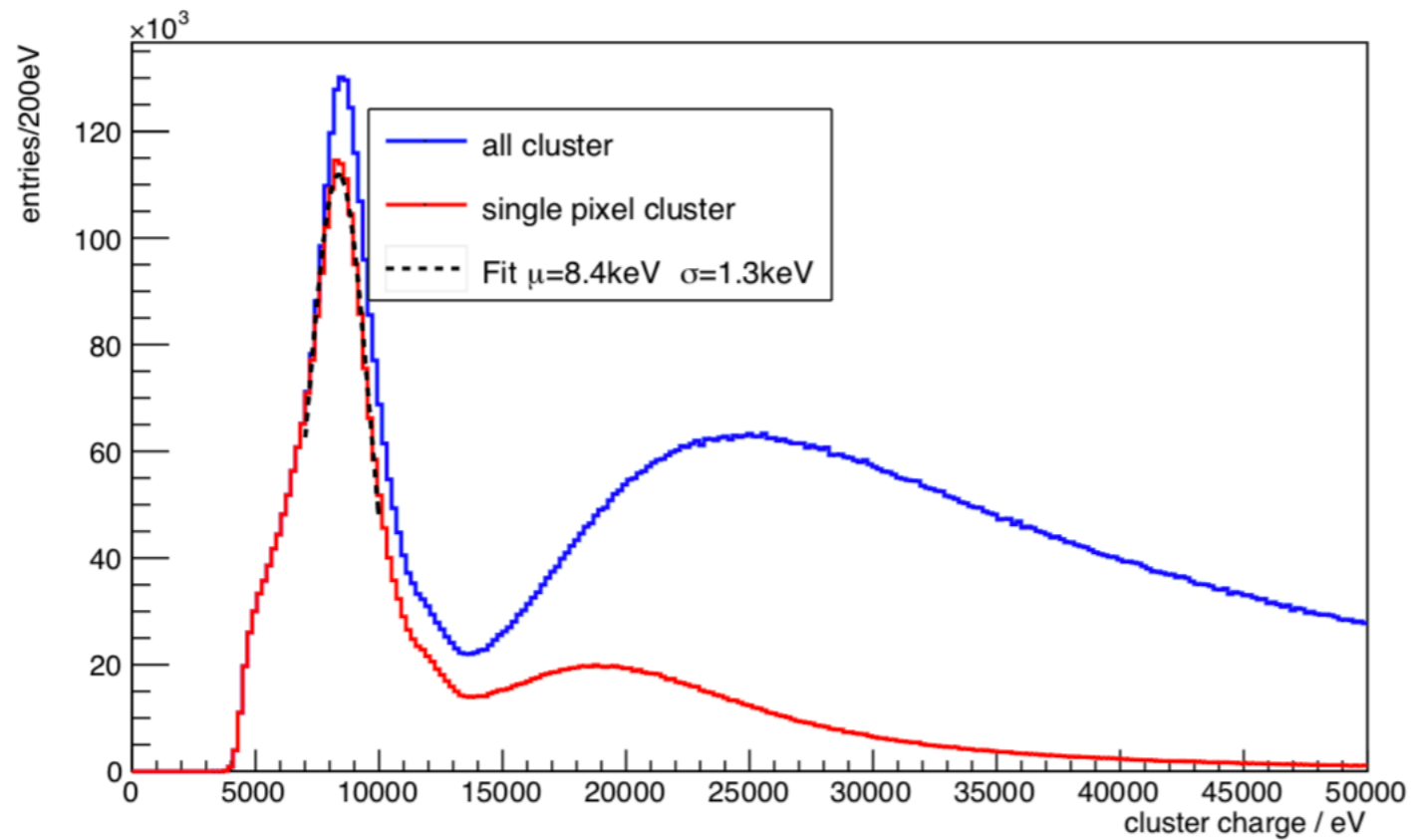
Pedestals



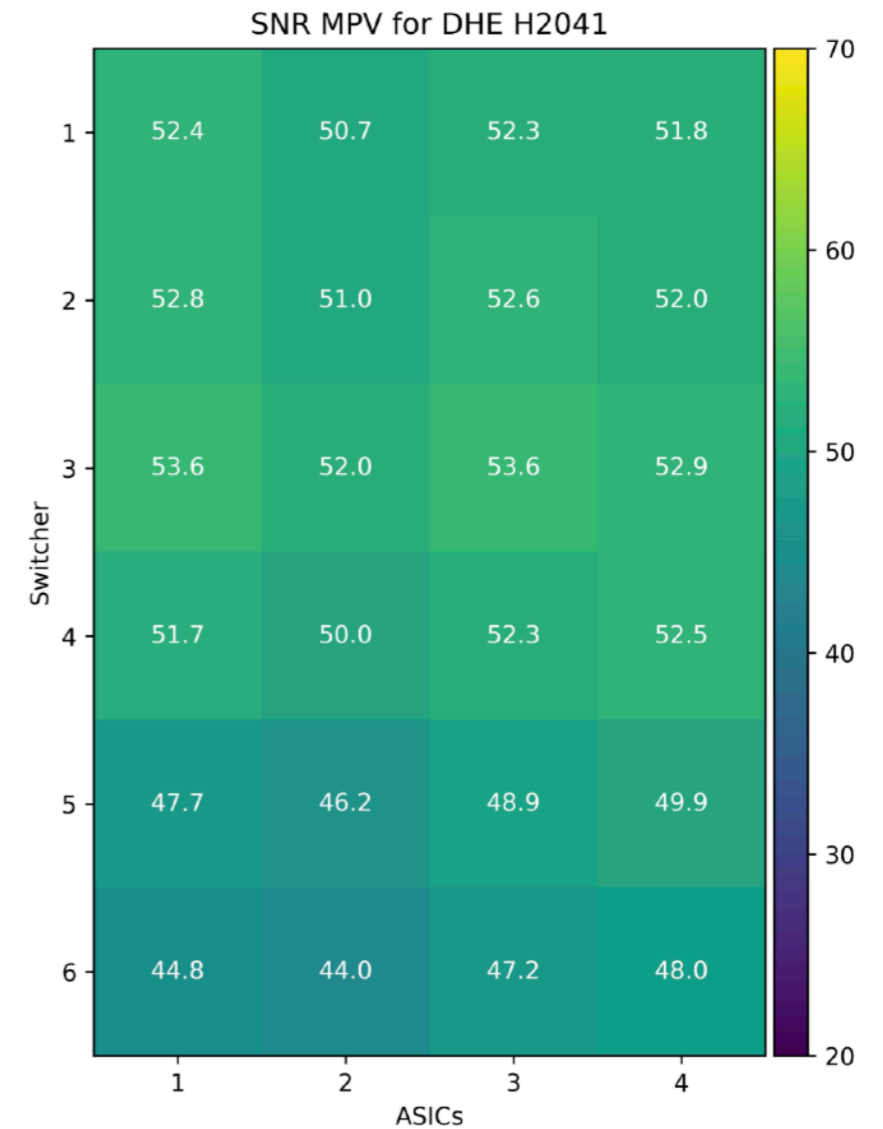
Principle of the offset compensation

Module Performance

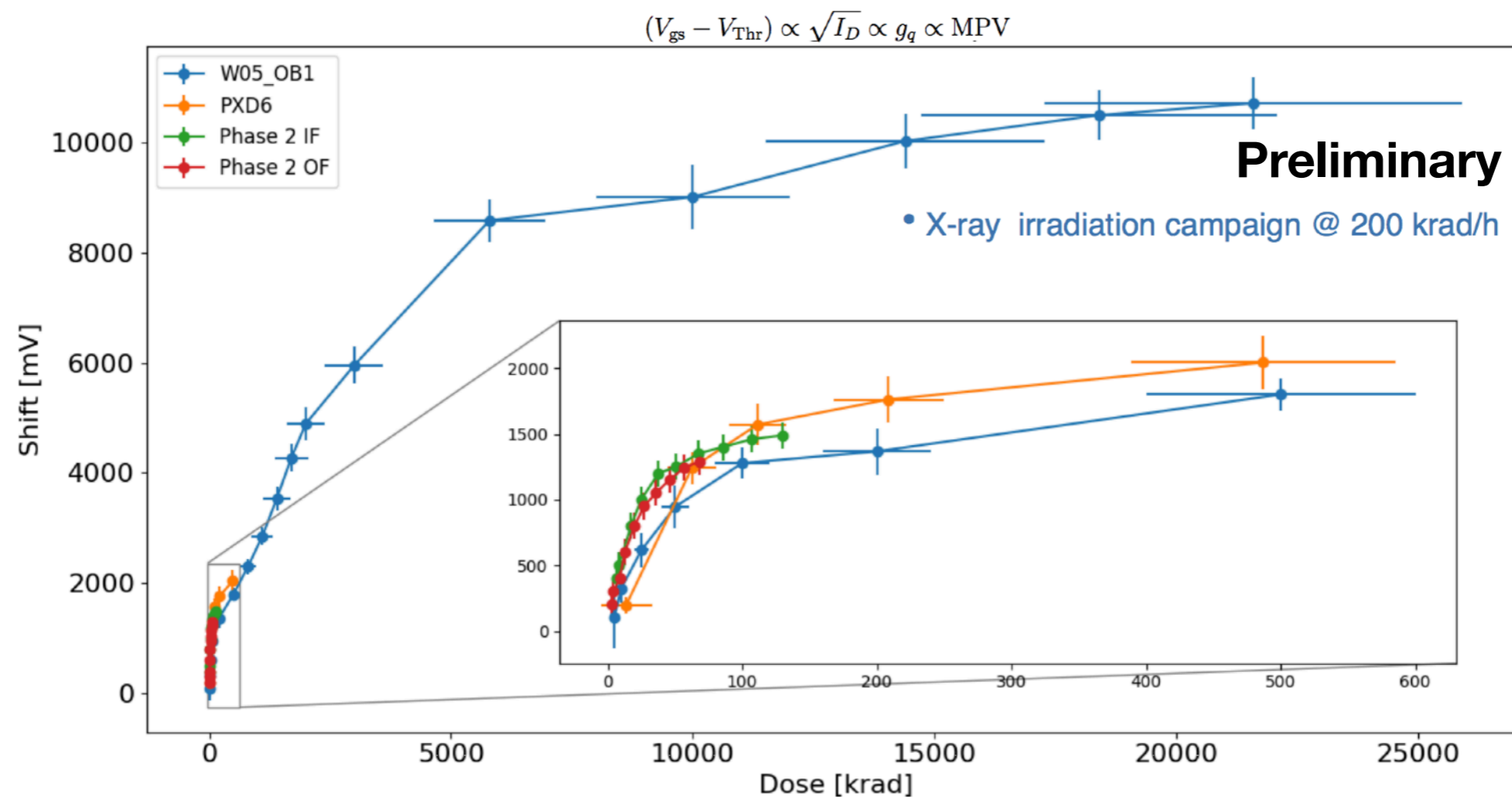
- ❖ Soft components (<10keV) on calibrated cluster energy spectra.
 - ❖ hint for synchrotron radiation



- ❖ SNR ≥ 50 has been achieved
 - ❖ from PXD Phase3 module



Irradiation test with full PXD module



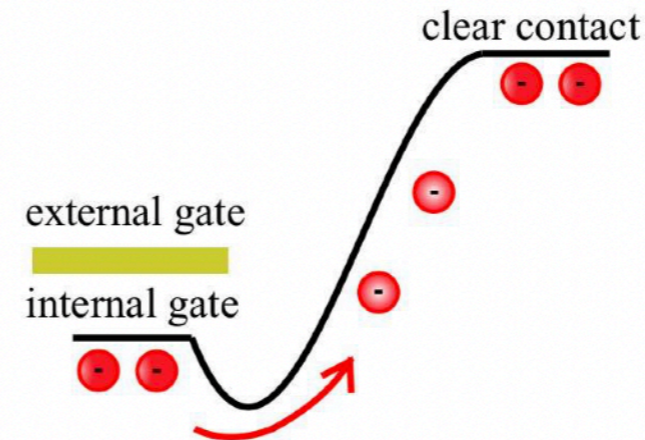
- ❖ Defects of SiO₂ cause shift of threshold voltage.
- ❖ Consistent results from dedicated irradiation campaign with earlier lab measurements and phase 2 experience
- ❖ Module still functional after > 25 Mrad (corresponding to 250mrad/s for 10 smy)

Gated Mode Operation

- ❖ At design luminosity we have to inject at 2x25Hz (\Rightarrow 20ms)
- ❖ Continuous / trickle beam injection causes noisy bunches.
- ❖ Sensor can be periodically blinded with Gated Mode (GM)
 - ❖ Newly created charges are not collected
 - ❖ Charges in internal gate are preserved

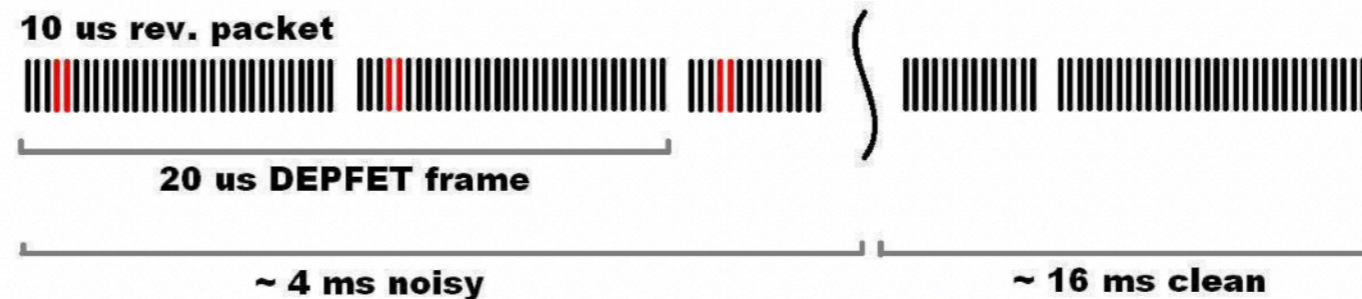
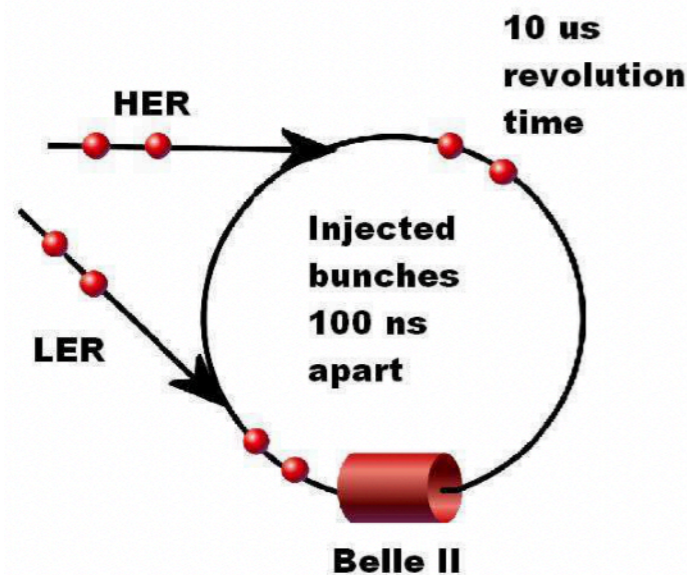
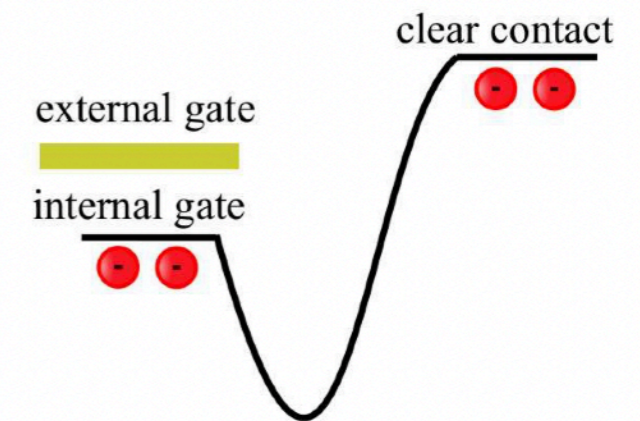
real clear

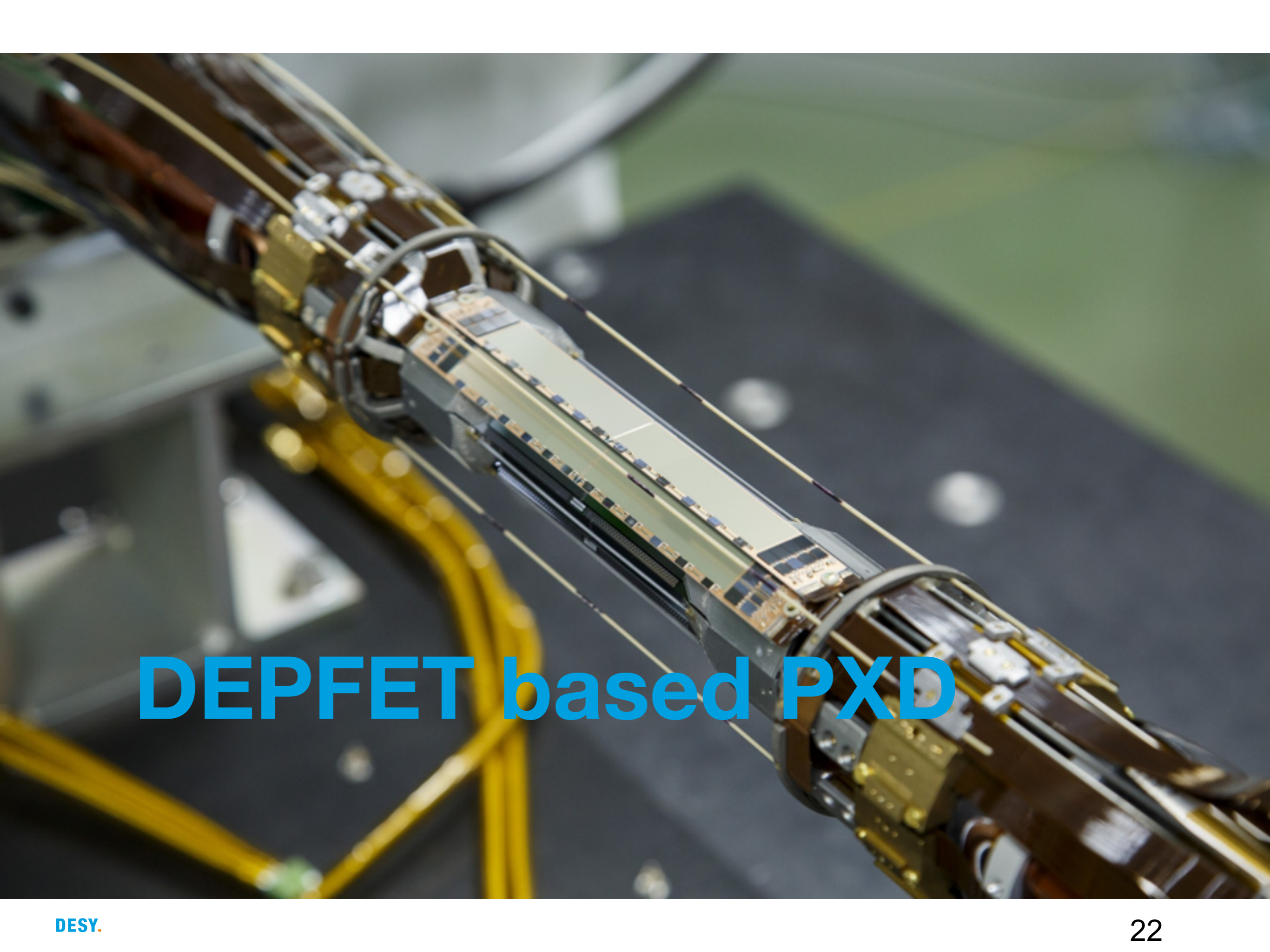
clear voltage high
gate voltage low



suppressed clear

clear voltage high
gate voltage high





DEPFET based PXD

PXD Layout

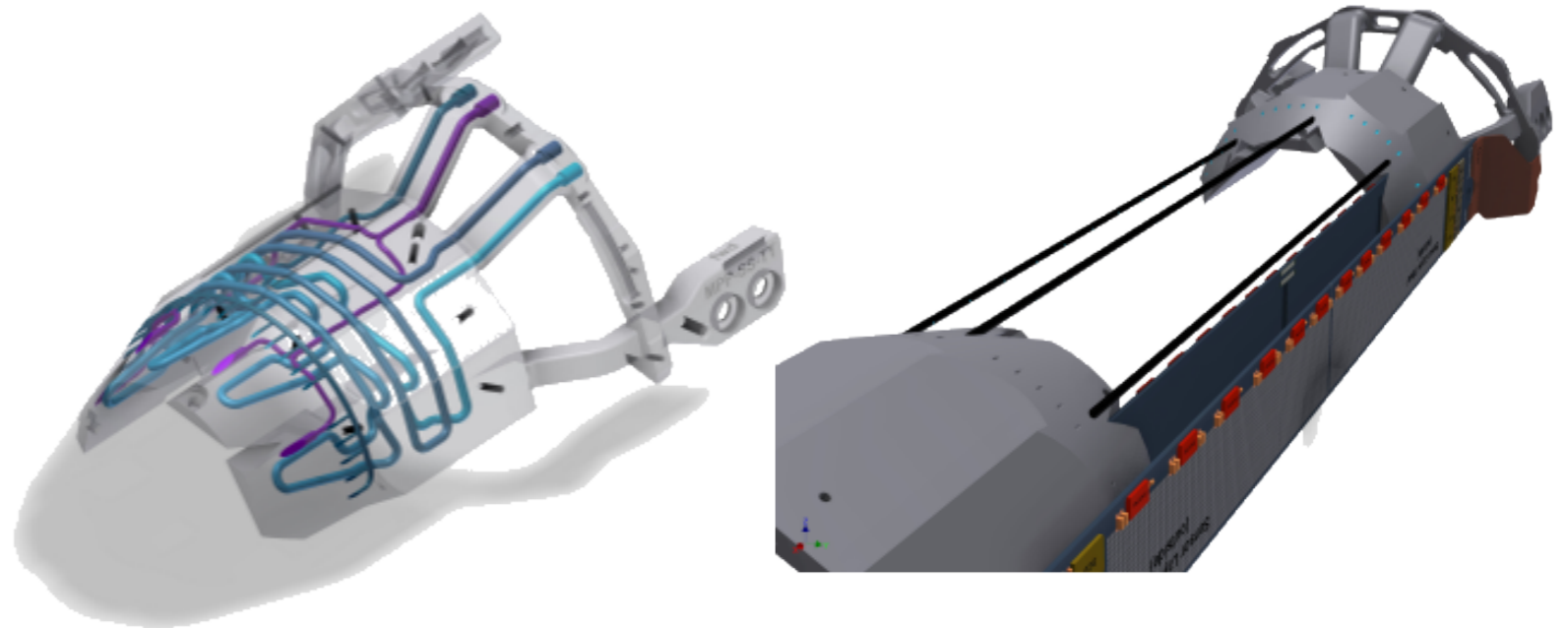
Ladder formed from 2 sensors

- ❑ self supporting
- ❑ 4 type of different sensors
- ❑ butt-face joint glueing, ceramic mini-rods embedded in the rim.



One common support for both layers

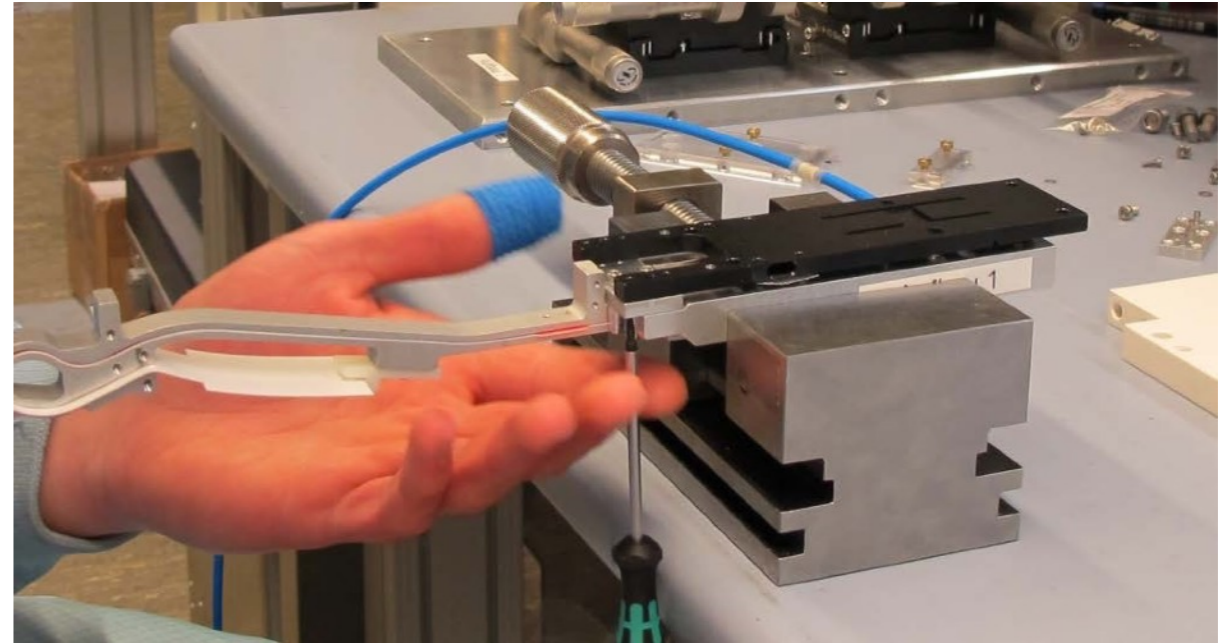
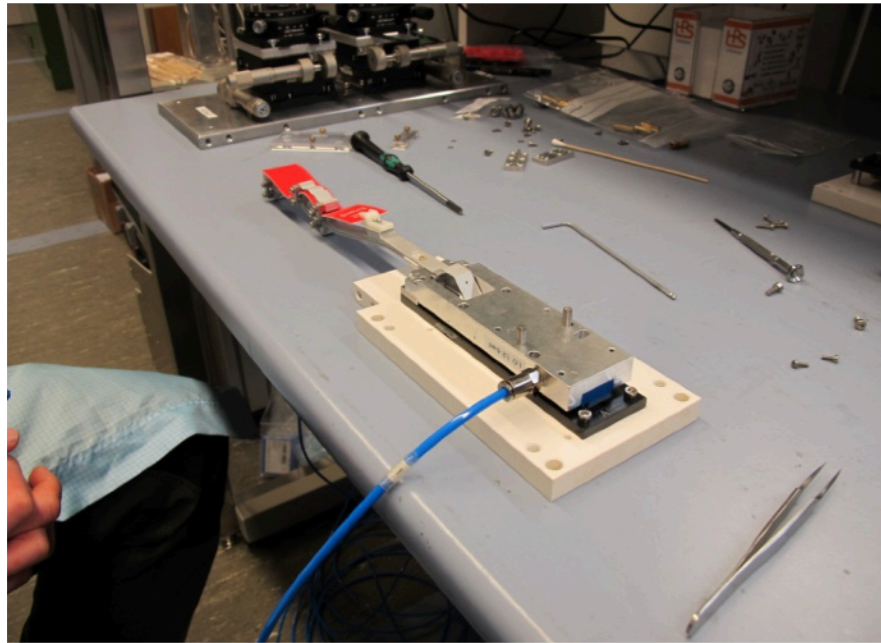
- ❑ 4 combined support and cooling blocks (SCBs)
- ❑ connected by silver coated carbon tubes for air cooling and grounding



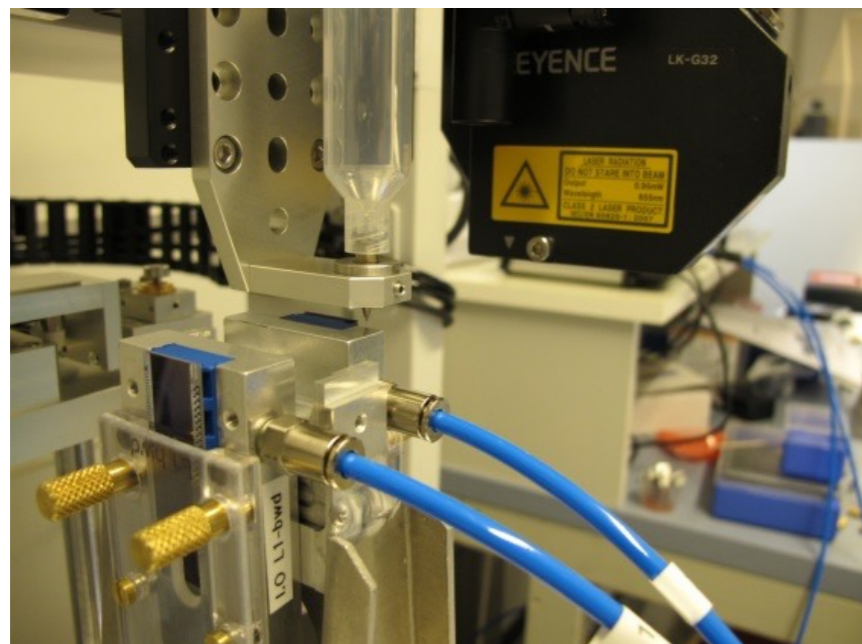
SCB, manufactured with 3D printing, with enclosed CO₂ and open N₂ channels integrated.

Ladder Gluing

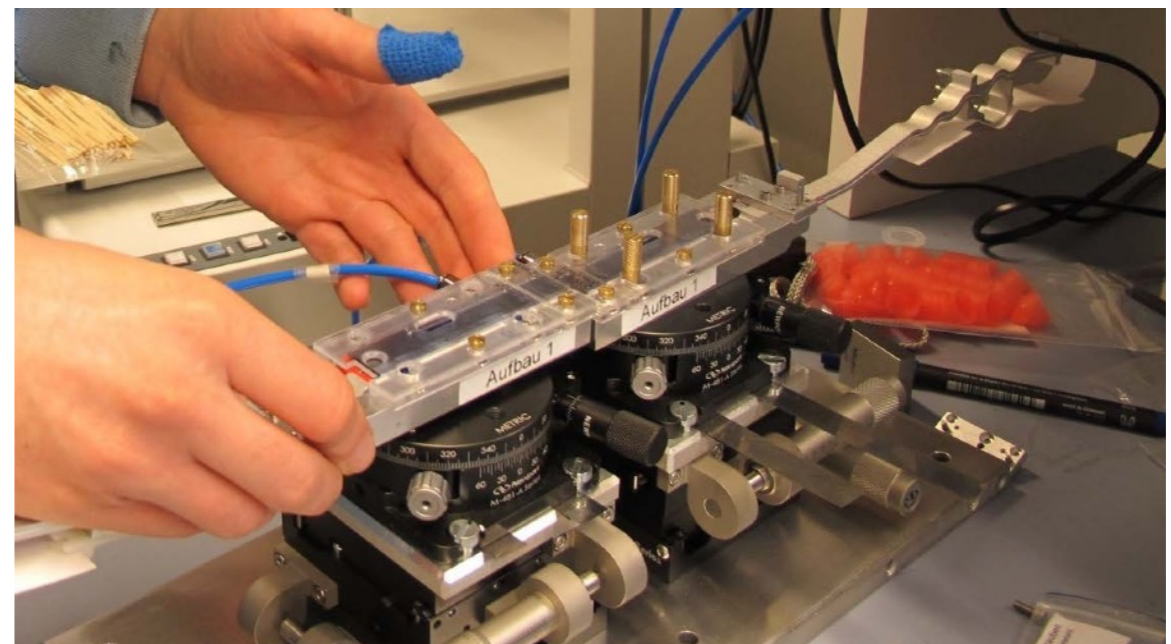
1. Preparations for Gluing Step



2. Glue automatically dispensed on sensor front edge

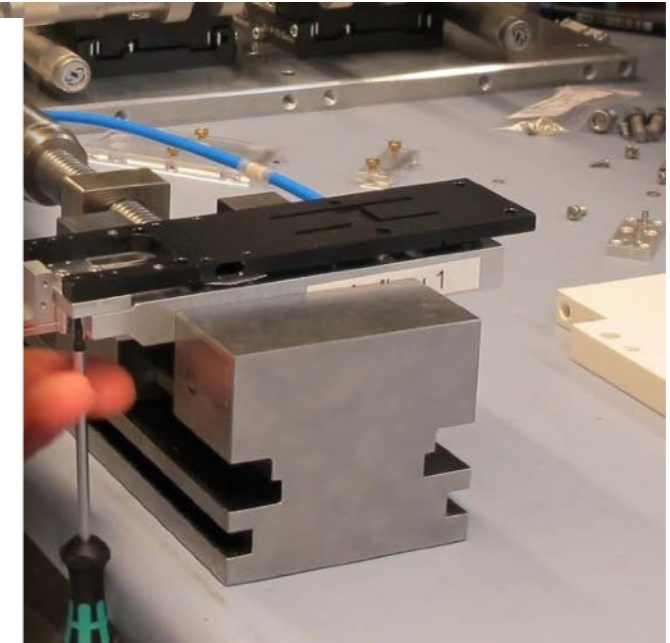
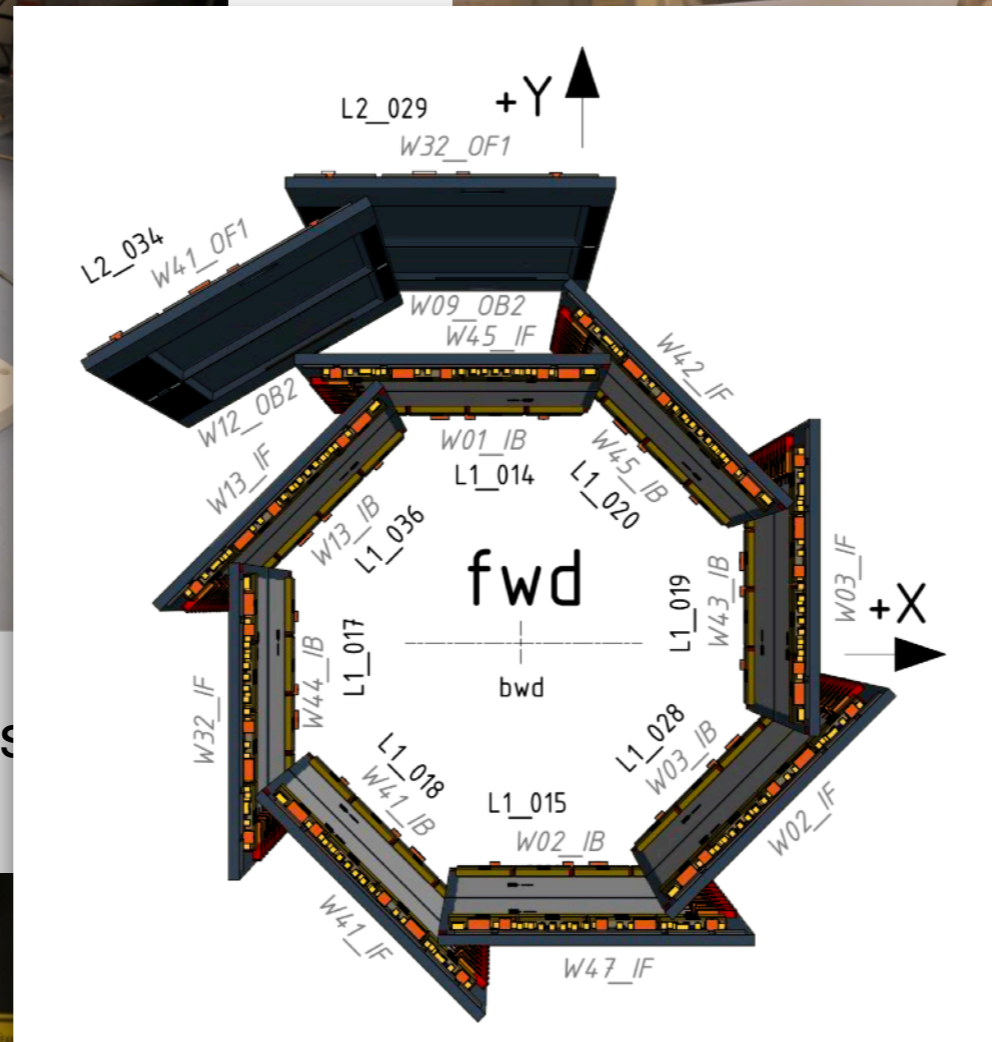
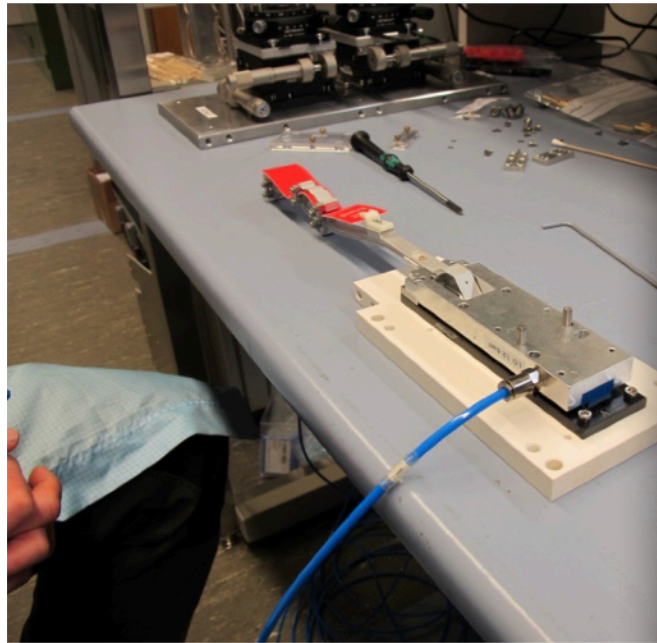


3. Modules placed on movable stages

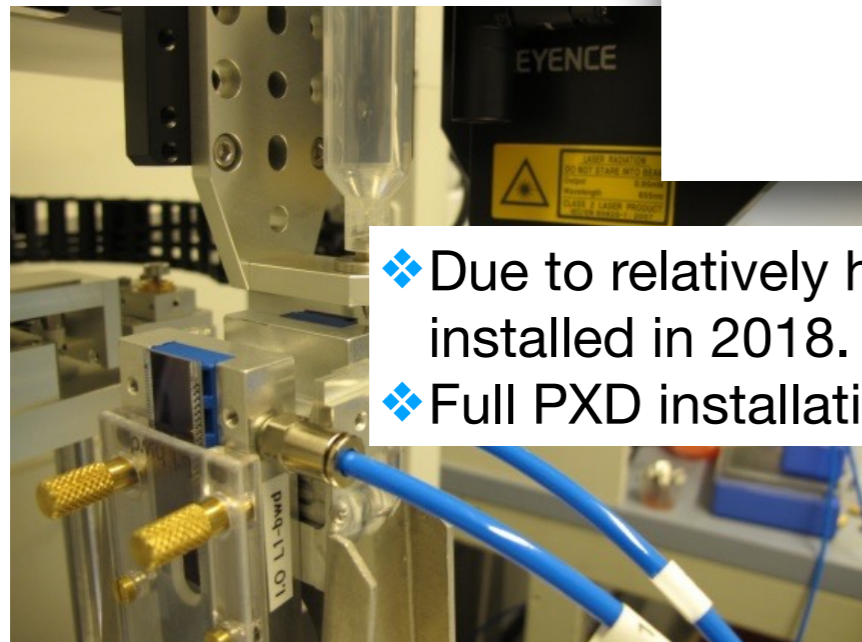


Ladder Gluing

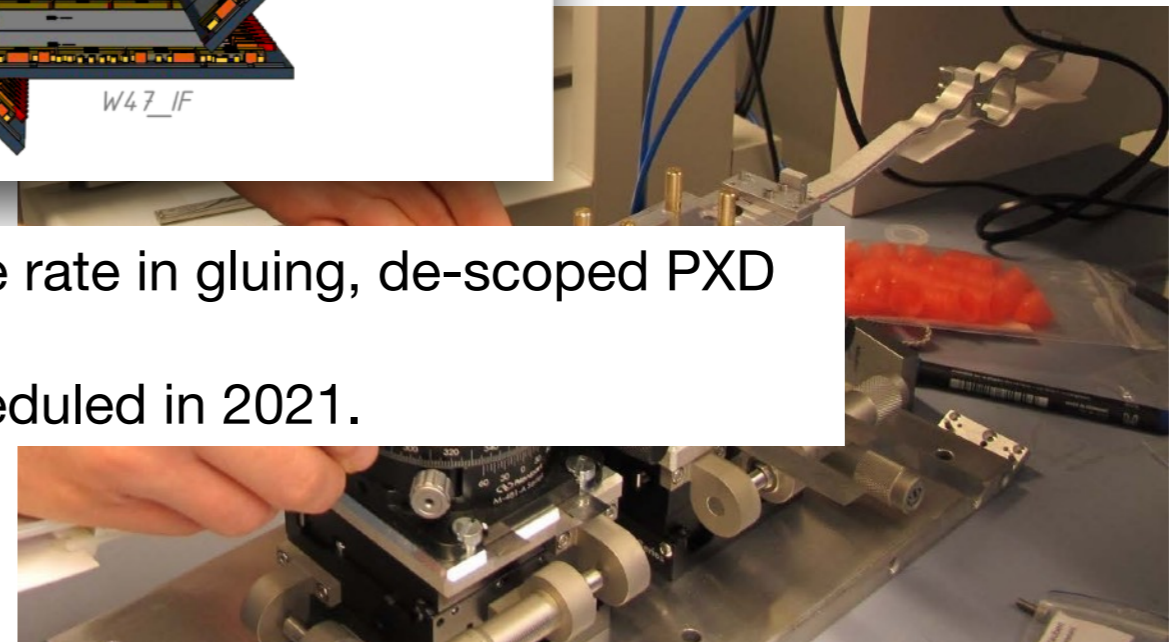
1. Preparations for Gluing Step



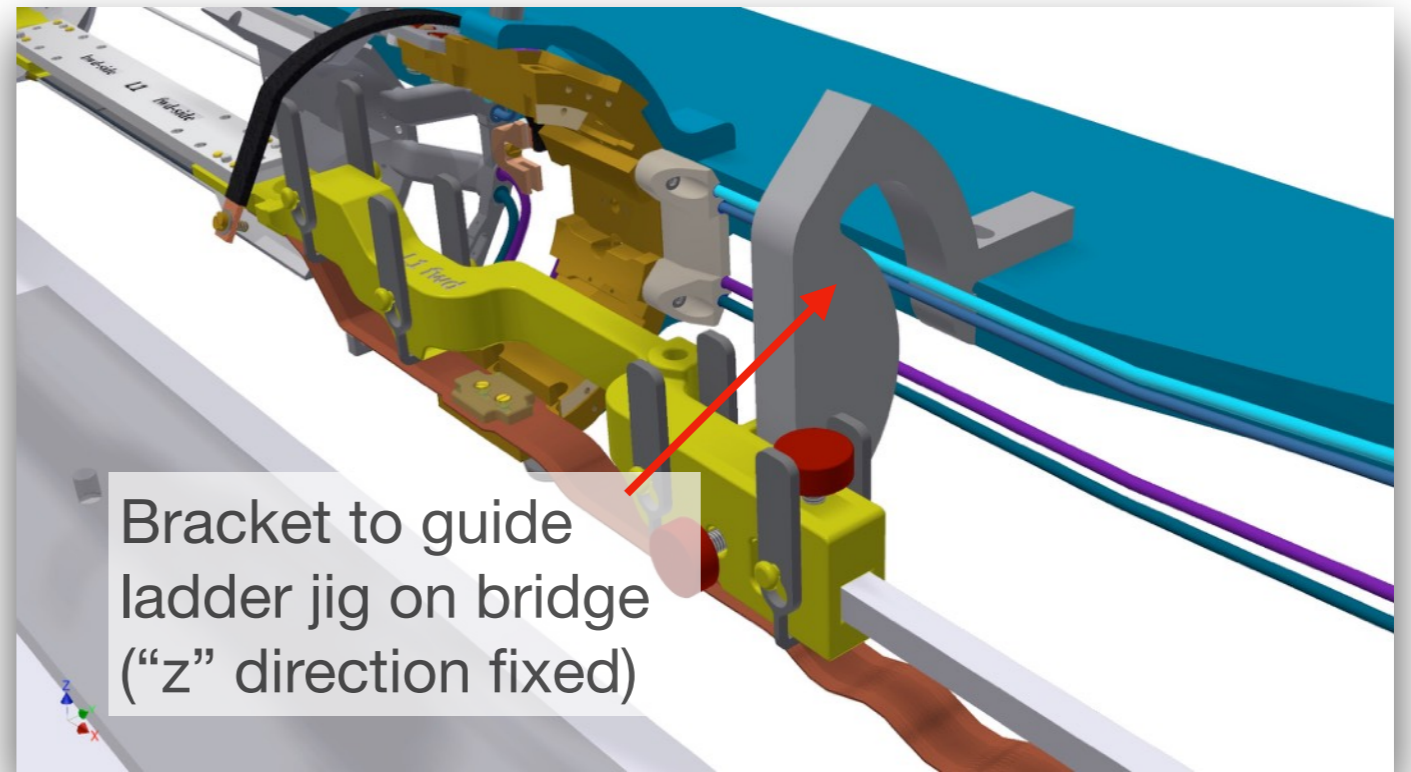
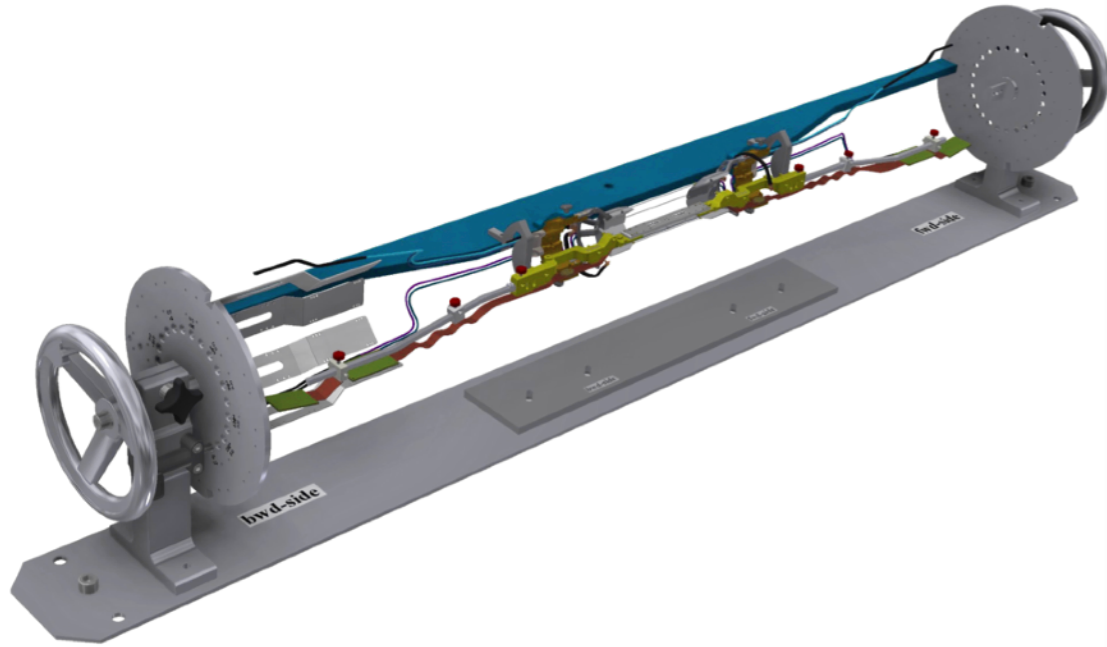
2. Glue automatically dispensed on sensor front edge



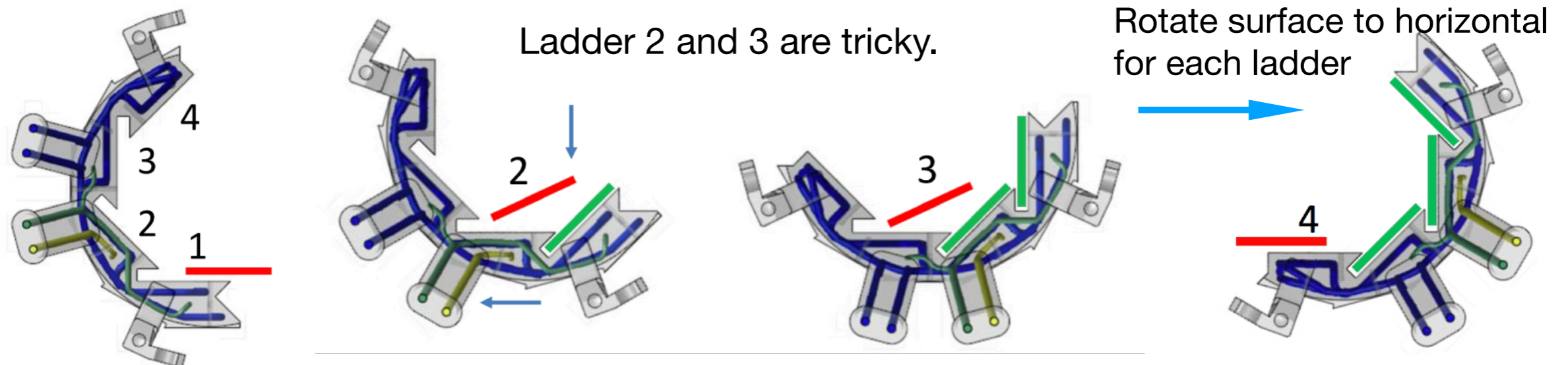
- ❖ Due to relatively high failure rate in gluing, de-scoped PXD installed in 2018.
- ❖ Full PXD installation is scheduled in 2021.



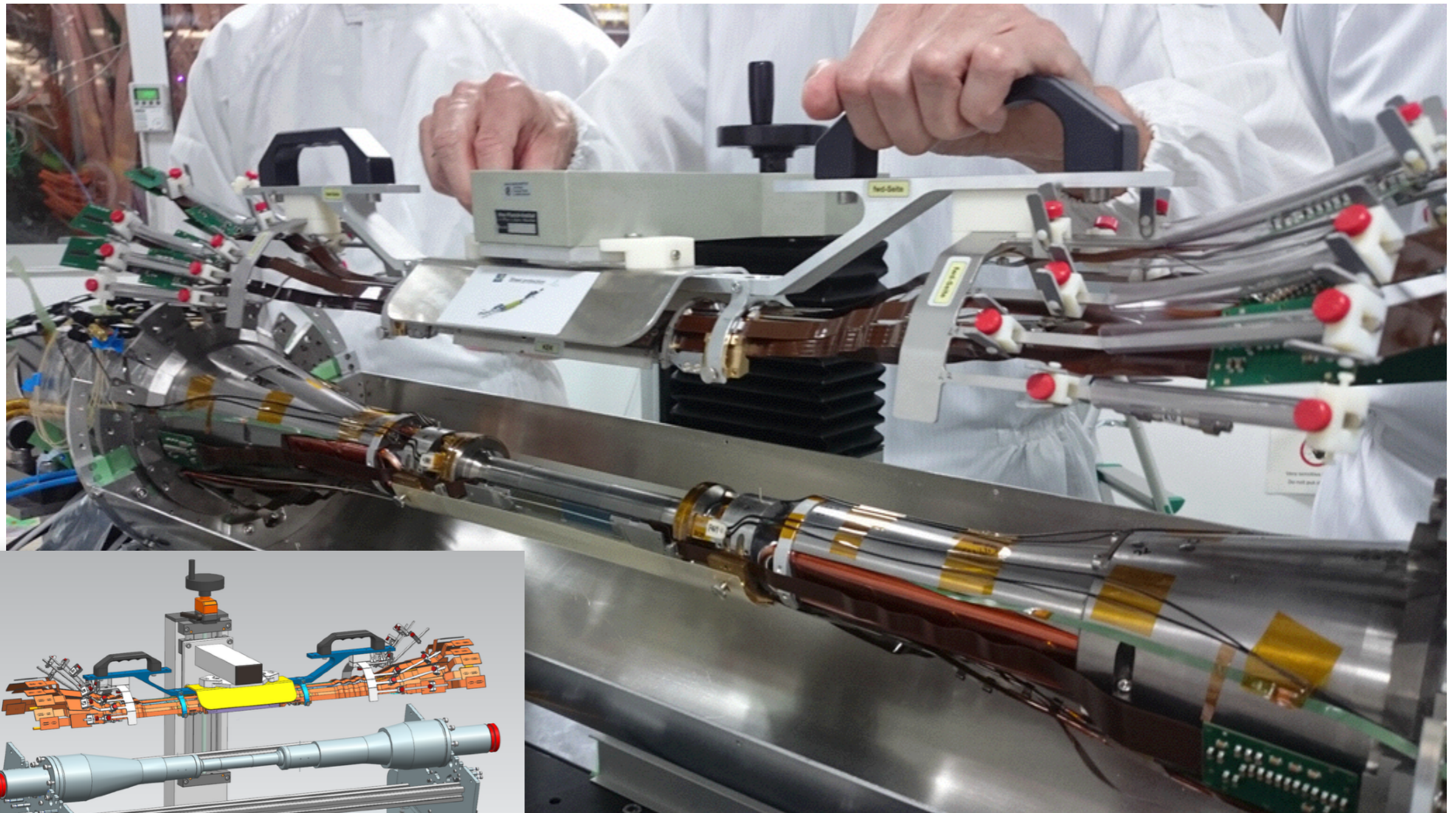
Ladder Mounting



- Mounting Sequence



Half-Shell Mounting

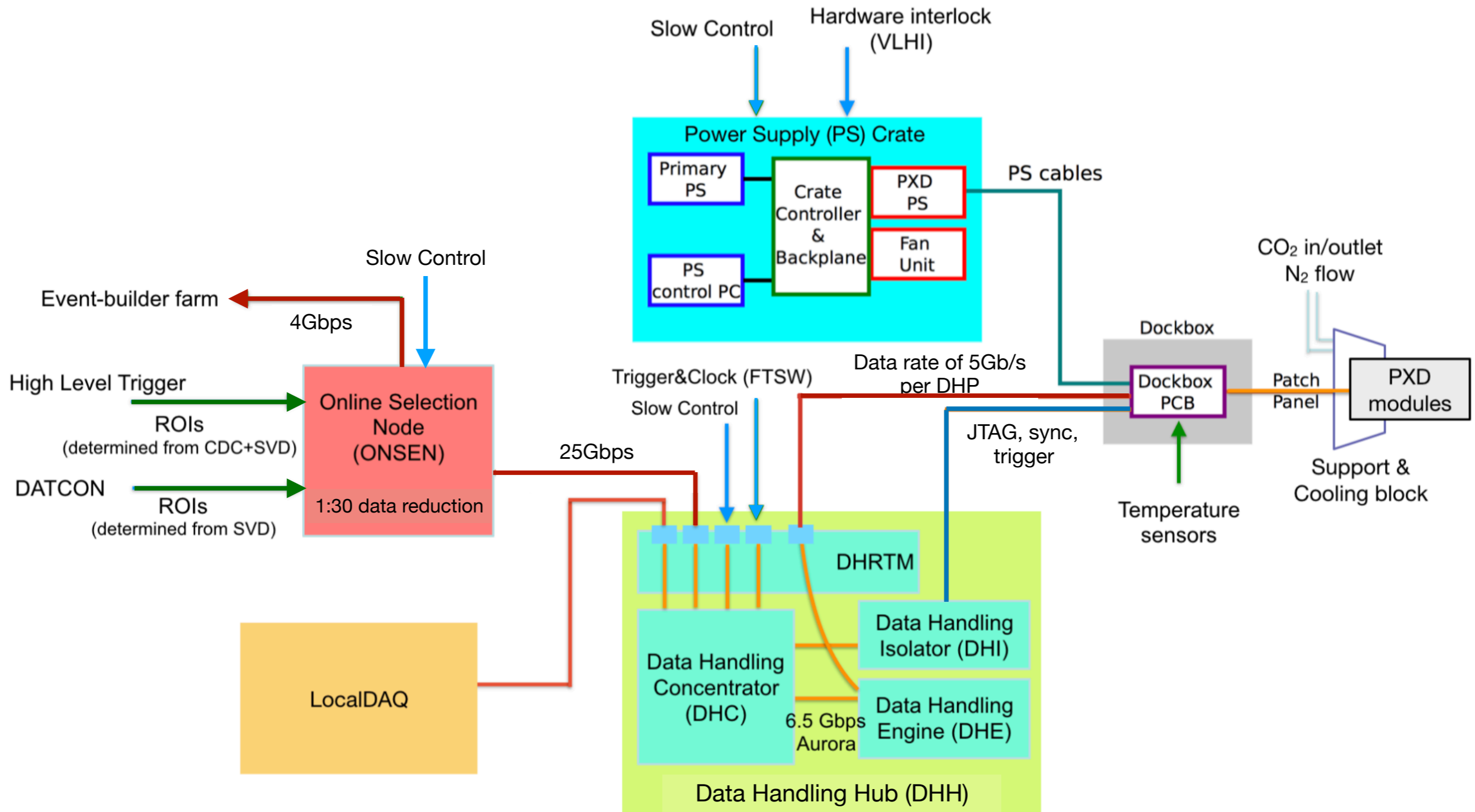




PXD in Belle II

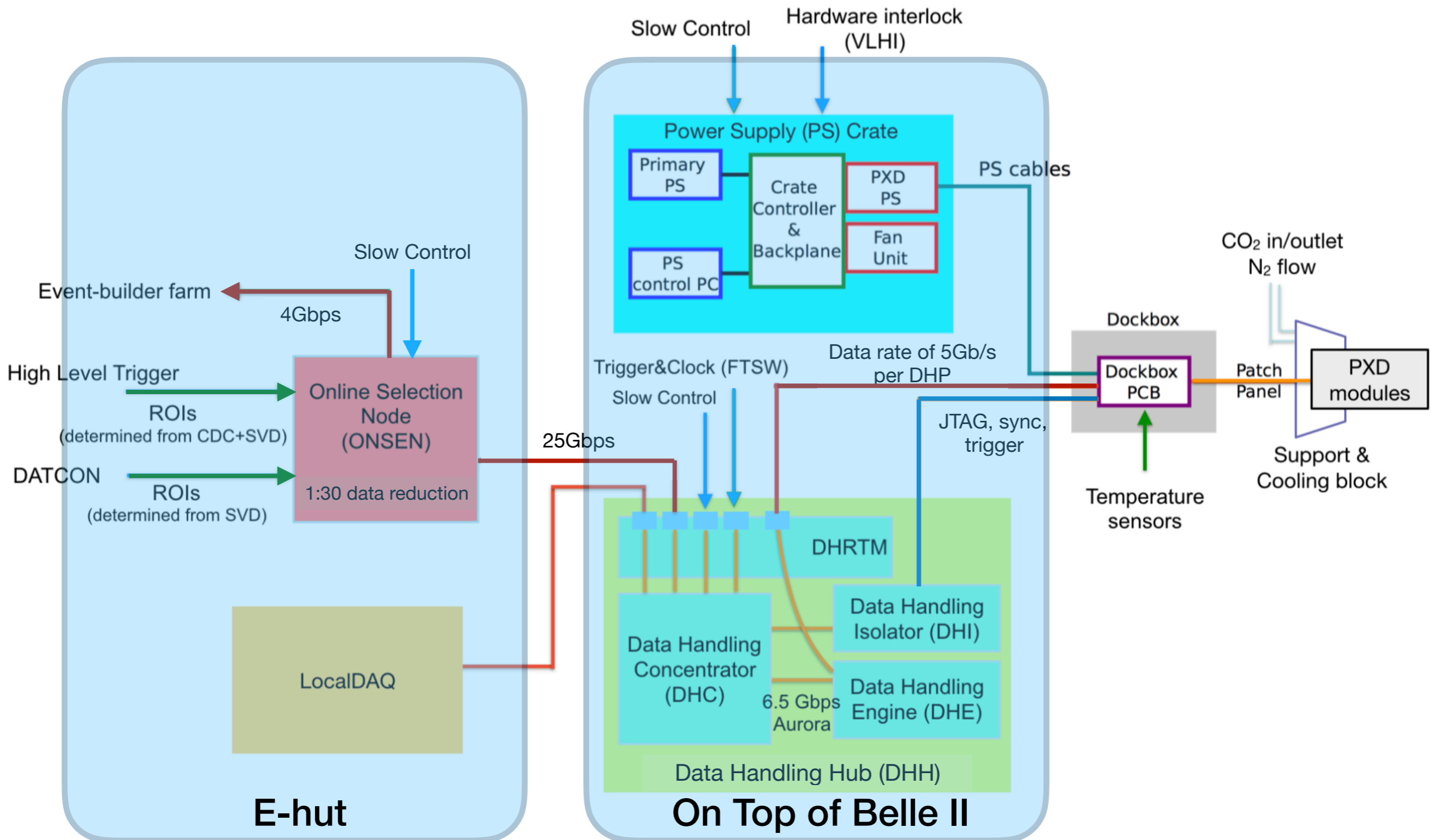
PXD System

Detector, service and readout

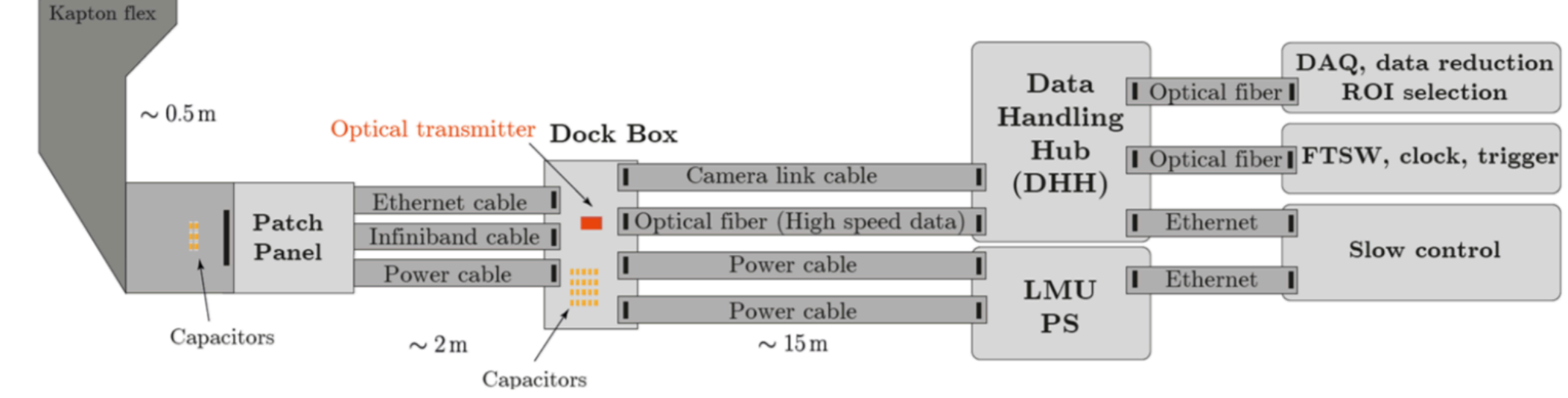
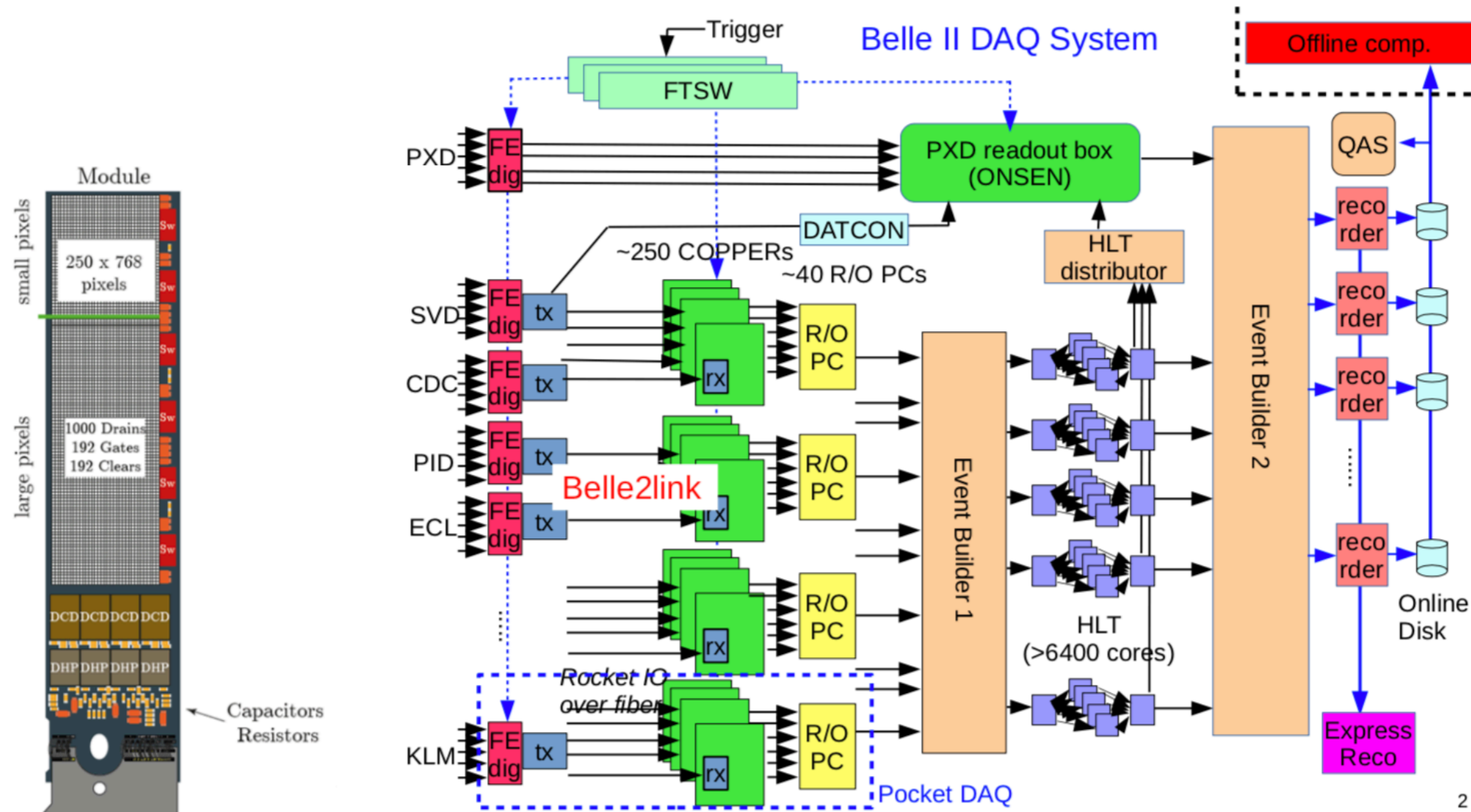


PXD System

Detector, service and readout



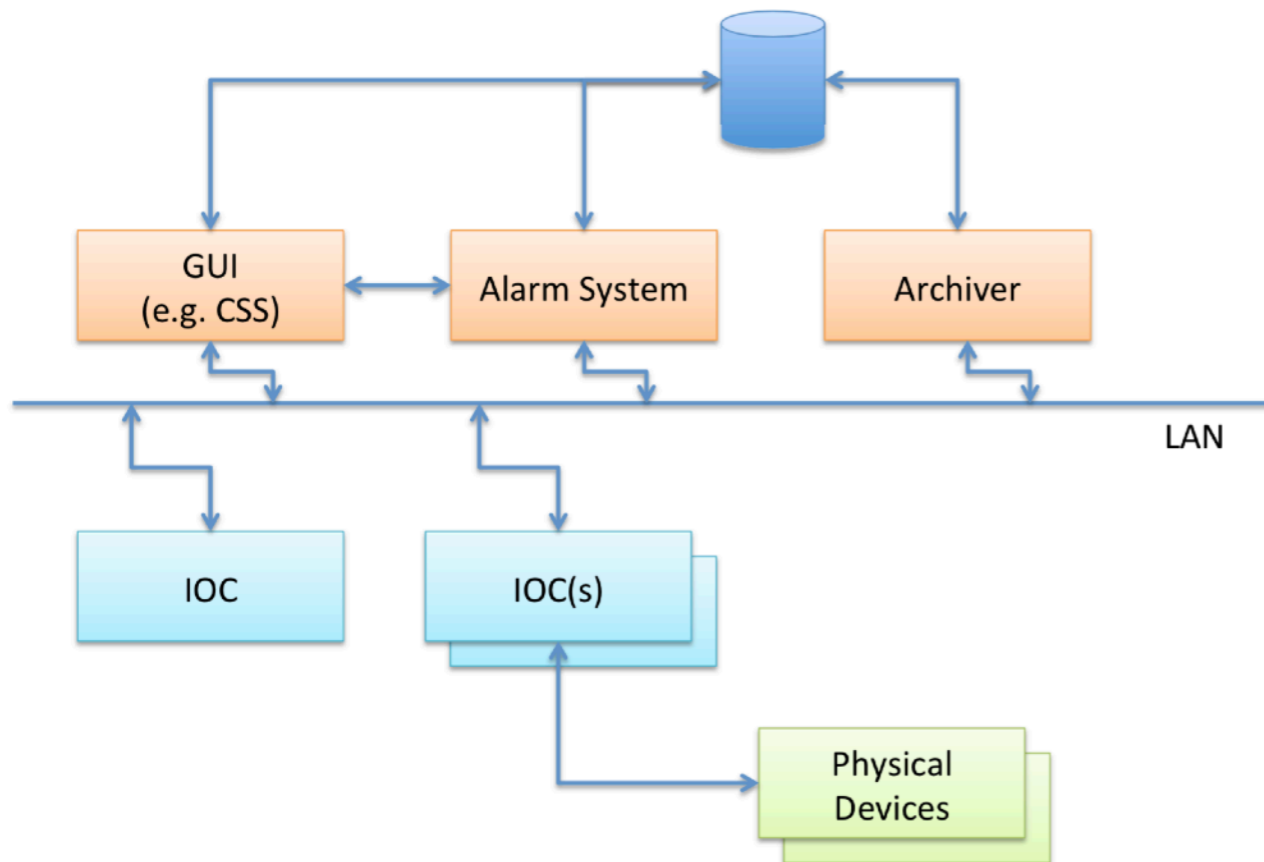
Global DAQ



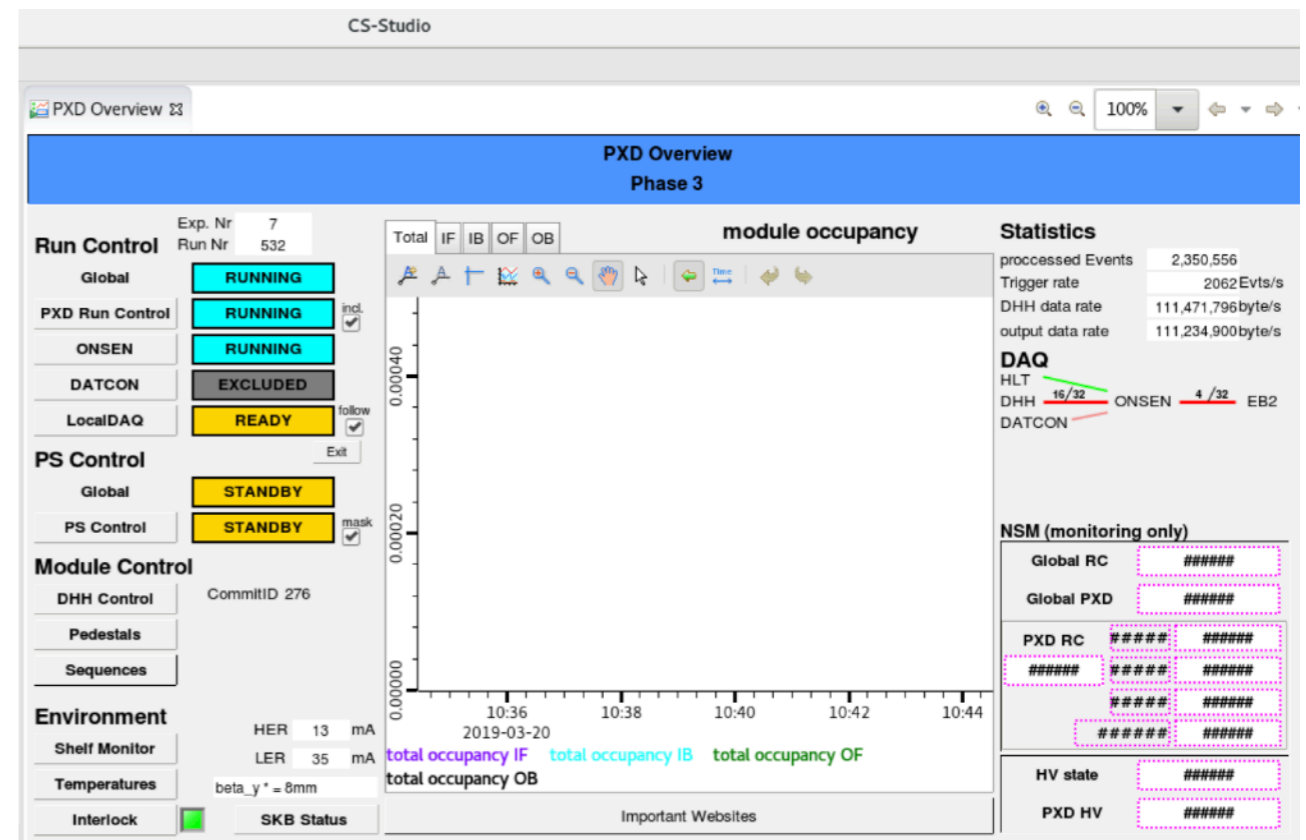
2

Slow Control

EPICS (Experimental Physics and Industrial Control System) Architecture



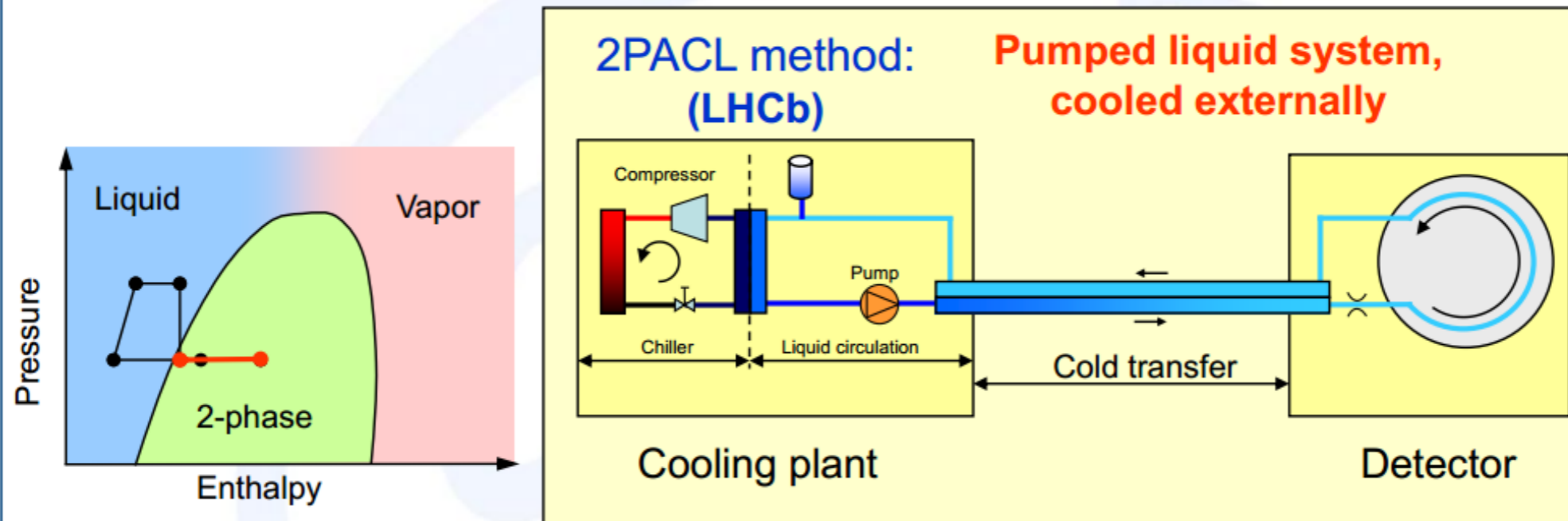
GUI: CS-studio



2-Phase CO₂ Cooling



New cycle for particle detectors: 2PACL (The 2-Phase Accumulator Controlled Loop)



- The 2PACL has the following advantages:
 - Cycle stays on the liquid side, no heat required (experiment can be cooled unpowered and no control heaters required)
 - Evaporator pressure=(temperature) controlled with a 2-phase vessel away from the experiment. No local control nor sensing needed!
 - All control hardware in a distant accessible cooling plant
 - Primary cooling can be anything, no accurate temperature control needed as long as it is colder than the 2PACL 2-phase temperature.
 - Inlet fluid state defined by physics => saturated liquid.
 - Large temperature range (typical from room temperature down to -40°C)

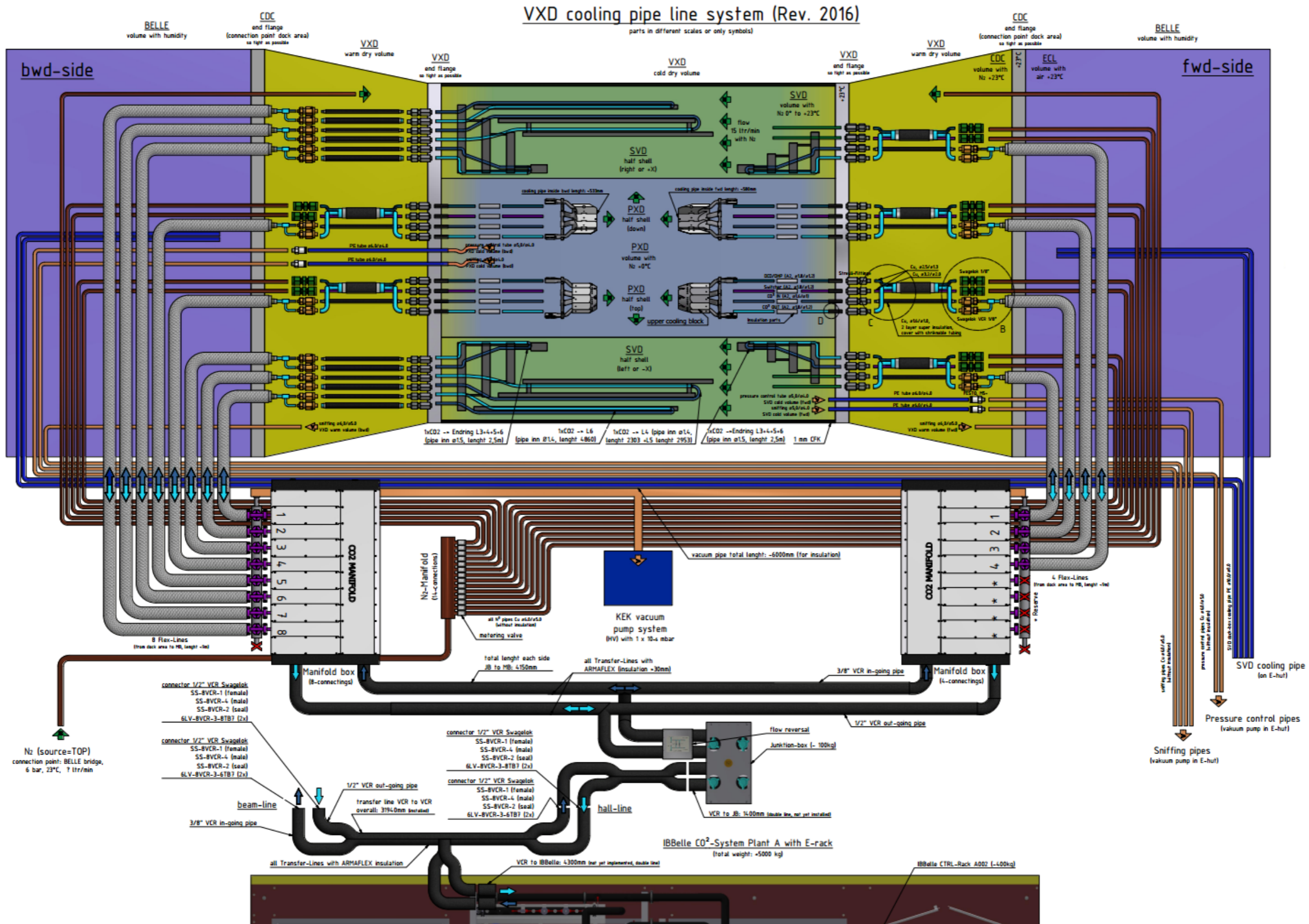
17

Challenges:

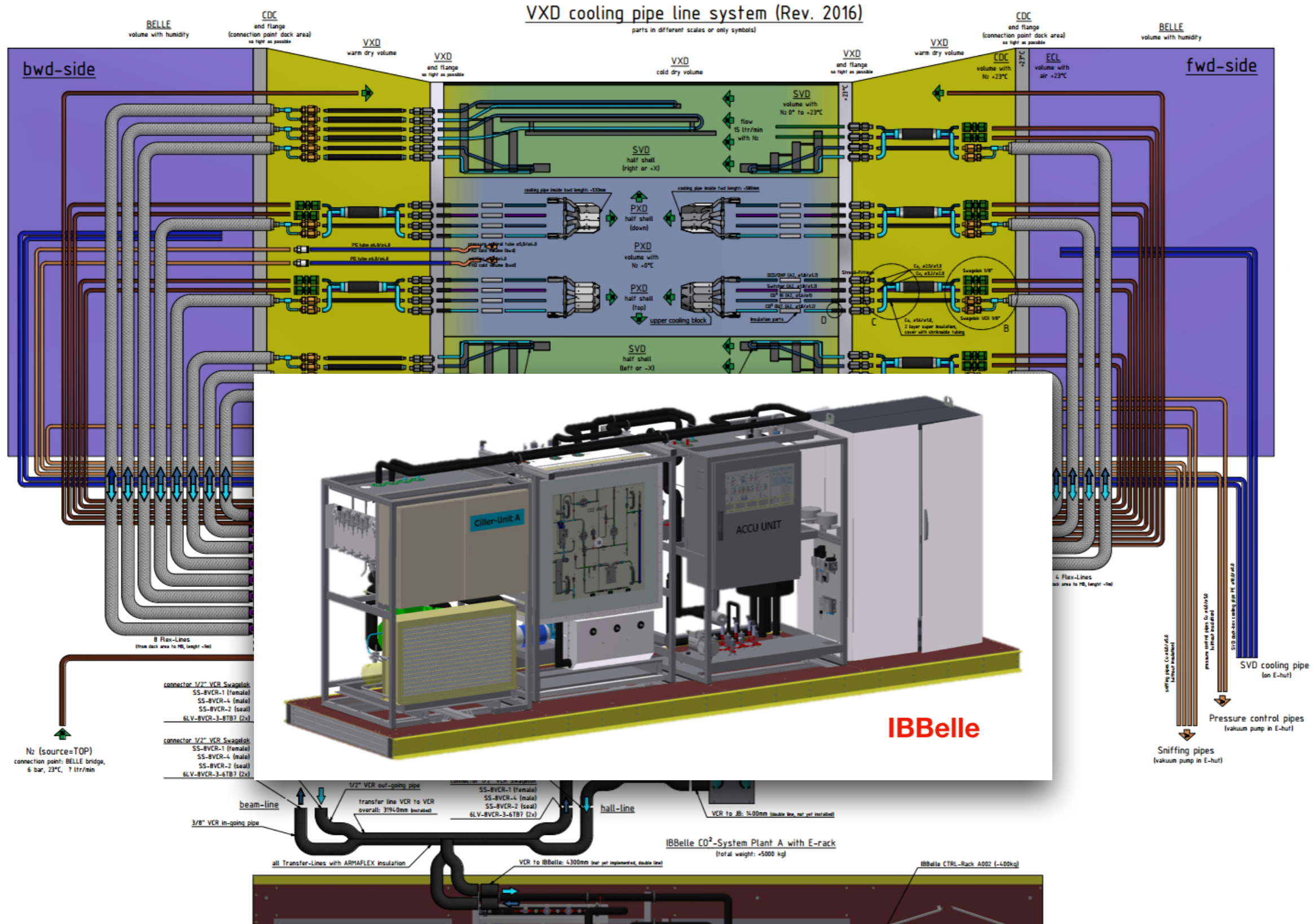
- ❖ high pressure
- ❖ need to guarantee the 2-phase state, otherwise “dry-out”.

From B. Verlaat, SLAC Advanced Instrumentation Seminars in March 2012

Belle II VXD Cooling Pipe Line System



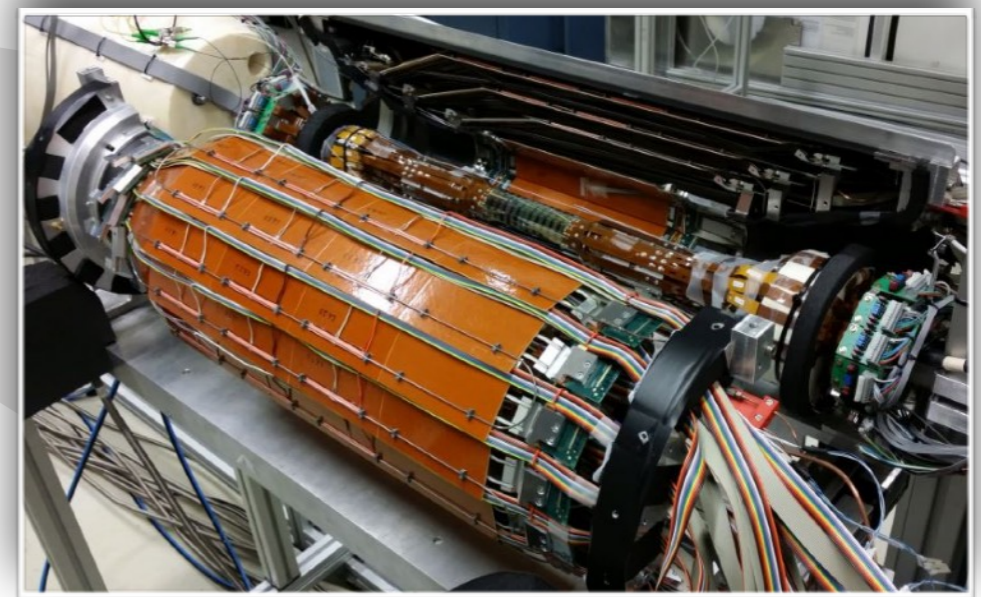
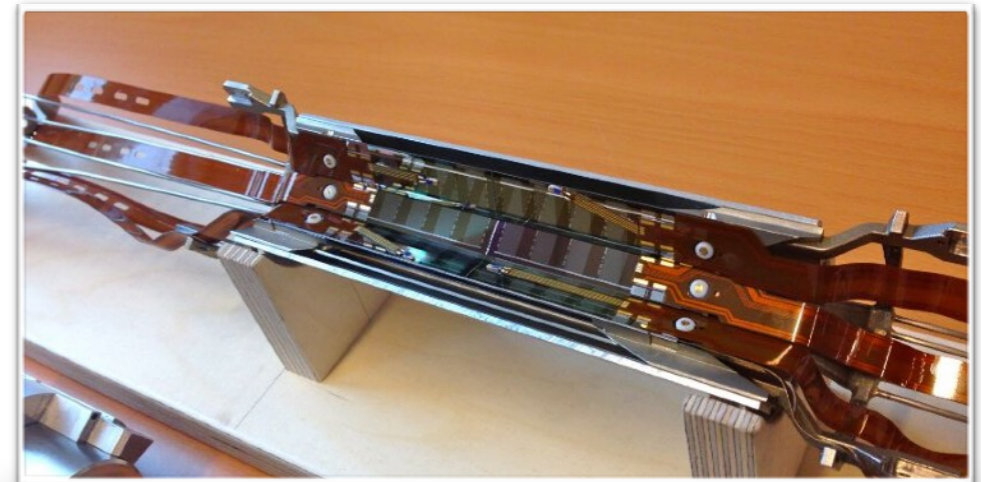
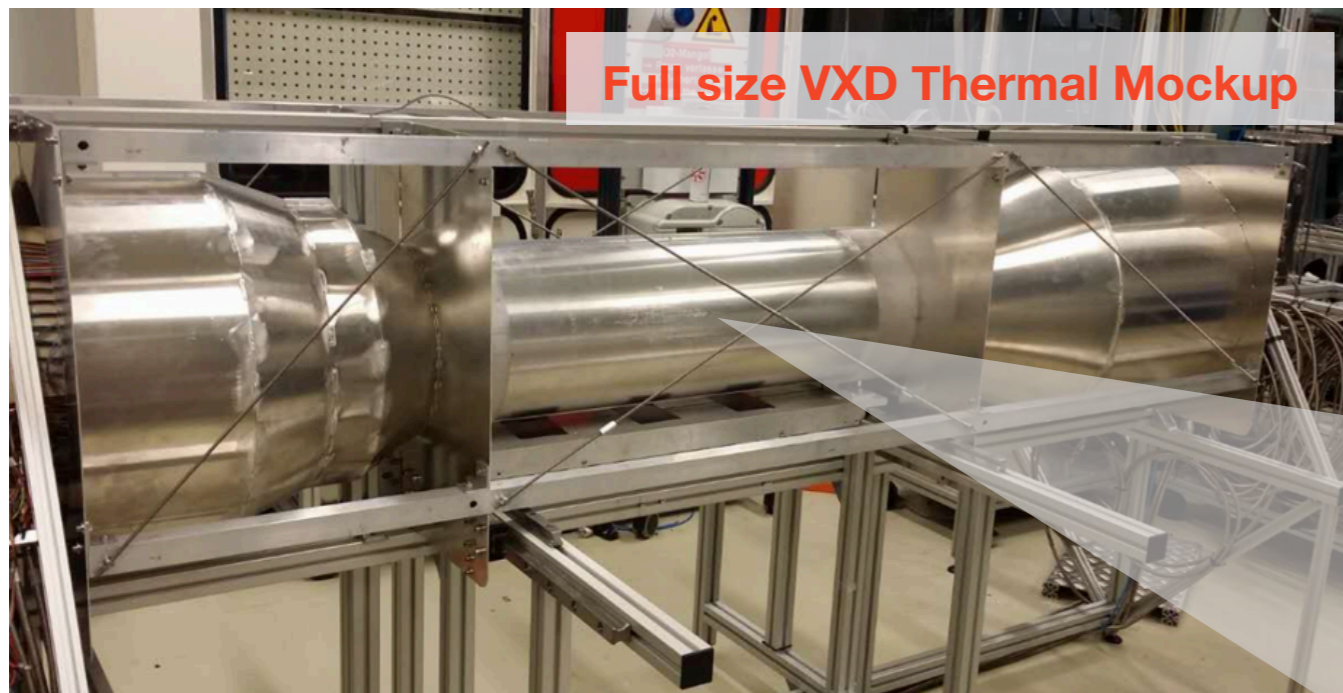
Belle II VXD Cooling Pipe Line System



VXD Thermal Mock-up @ DESY

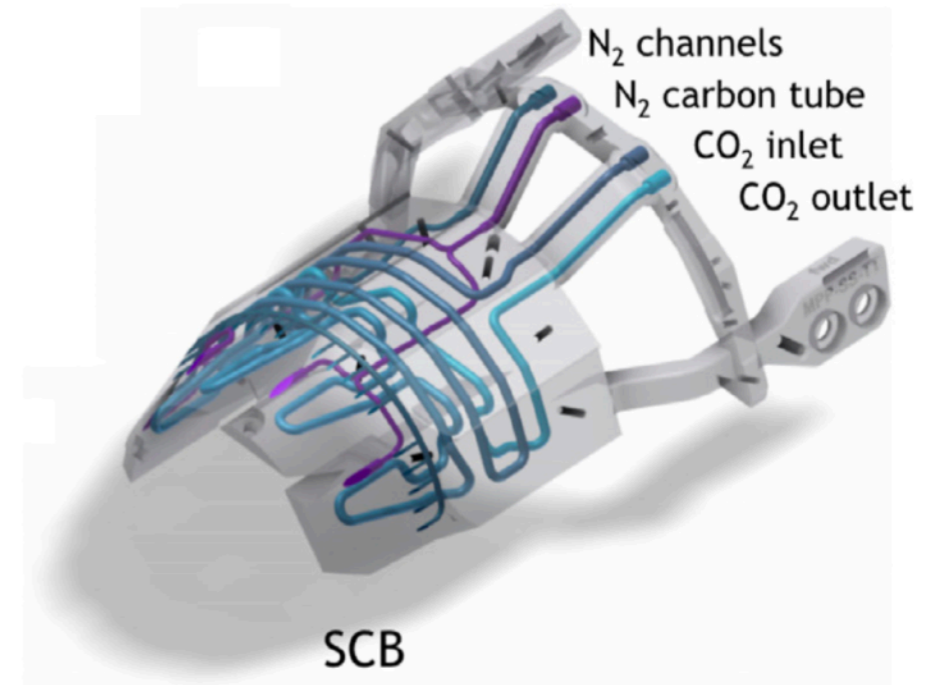
Study the thermal / mechanical properties of VXD as well as the integration procedures.
Verify the performance of the 2-phase CO₂ cooling system.

- ❖ The temperature on sensors and ASICs need to be well controlled for S/N improvement.
- ❖ A cooling capacity of 2-3kW in the dense VXD volume is required.
- ❖ The 2-phase CO₂ cooling is an efficient concept for low-mass detector.
- ❖ An optimal CO₂ temperature region of -20 to -30°C has been established.

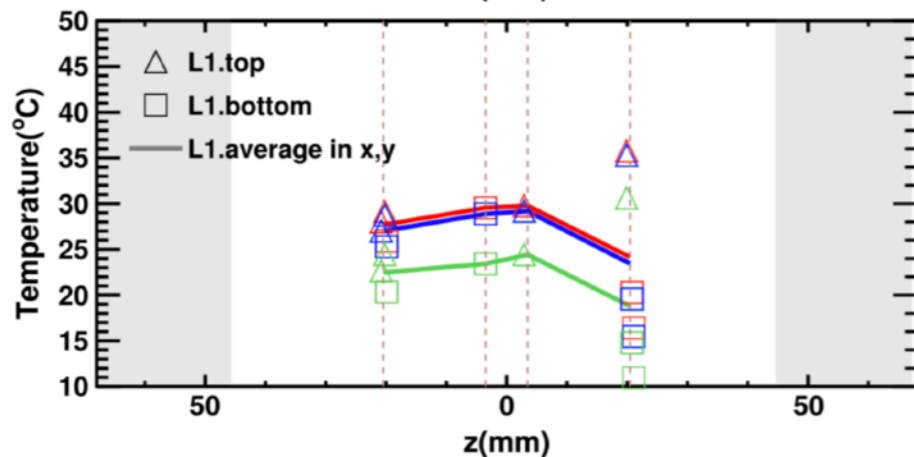
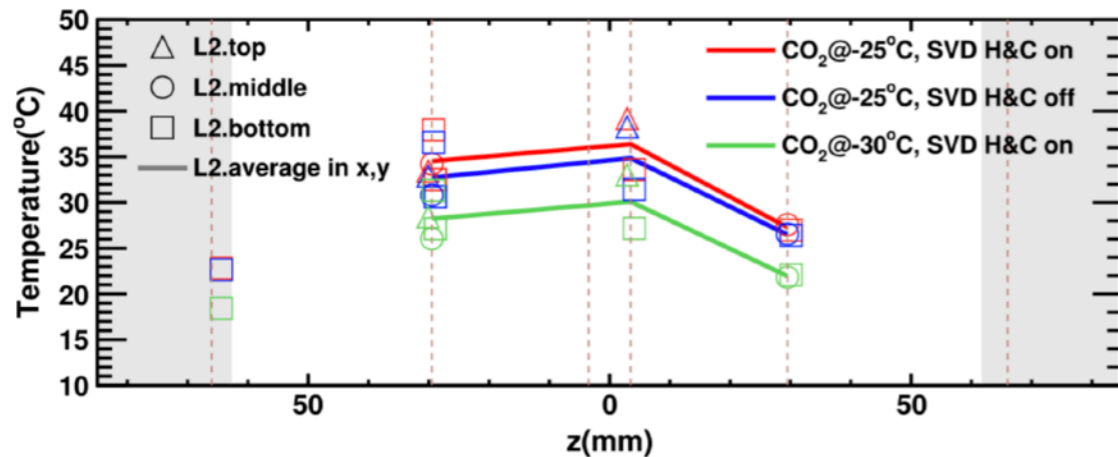


Temperature along PXD Ladder

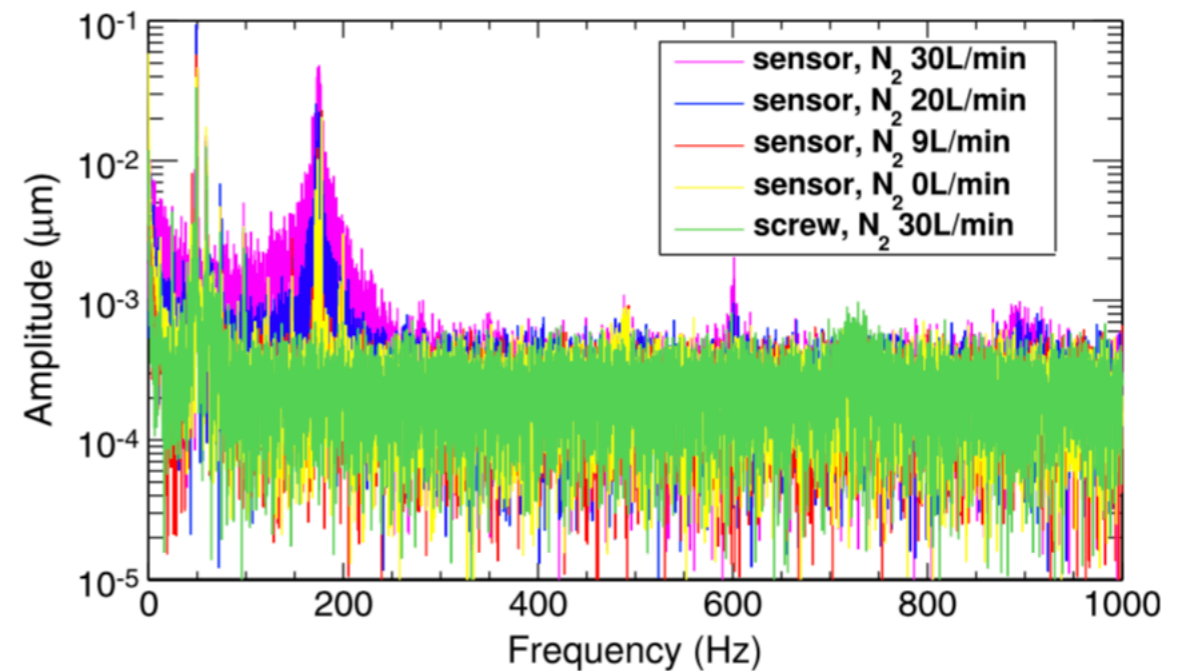
- ❖ The power consumption of full PXD is 420W,
 - ❖ 360W are contributed from DCD/DHP, which are located in the end of stave.
 - ➔ Active 2 phase CO₂ cooling is required there.
 - ❖ Little power derived from matrix (0.5W per module) and Switchers (1W per module)
 - ➔ Forced N₂ cooling is sufficient in the sensitive area.



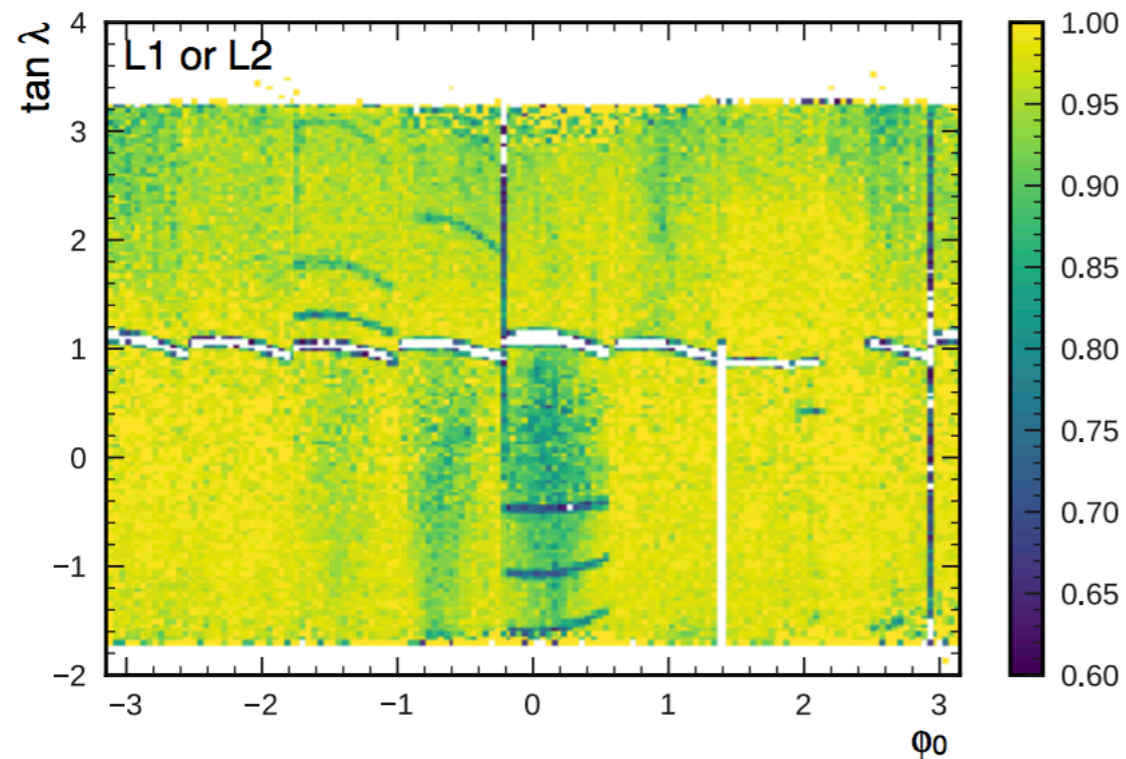
Temperature along PXD ladder



Possible vibration in PXD ladder

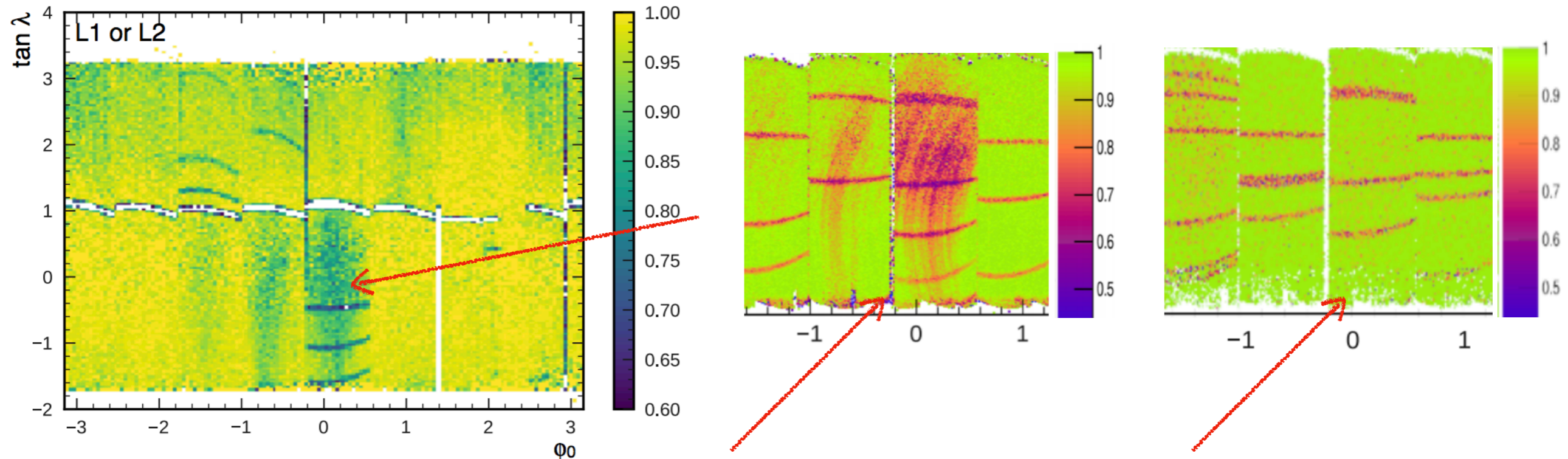


PXD Performance: Efficiency



- ❖ Projection on the ϕ_0 - $\tan(\lambda)$ plane.
- ❖ $\lambda \equiv \pi/2 - \theta$, : angle between a track and the plane \perp to the beam.
- ❖ Gaps between fwd & bwd modules and between half shells
- ❖ Few modules not yet at optimal working point

PXD Performance: Efficiency



Ring structures indicate shift of working point

- ❖ The rings due to small scale variations in the bulk doping.
- ❖ Almost completely invisible if properly biased.

Voltages were adjusted to cure the rings

- ❖ Projection on the ϕ_0 - $\tan(\lambda)$ plane.
- ❖ $\lambda \equiv \pi/2 - \theta$, : angle between a track and the plane \perp to the beam.
- ❖ Gaps between fwd & bwd modules and between half shells

Transverse Impact Parameter (d_0) Resolution

- ❖ After correcting for the beam spot position, the ϕ -dependent $\sigma(d_0)$ depends on the intrinsic VXD resolution and transverse size of the luminous region:

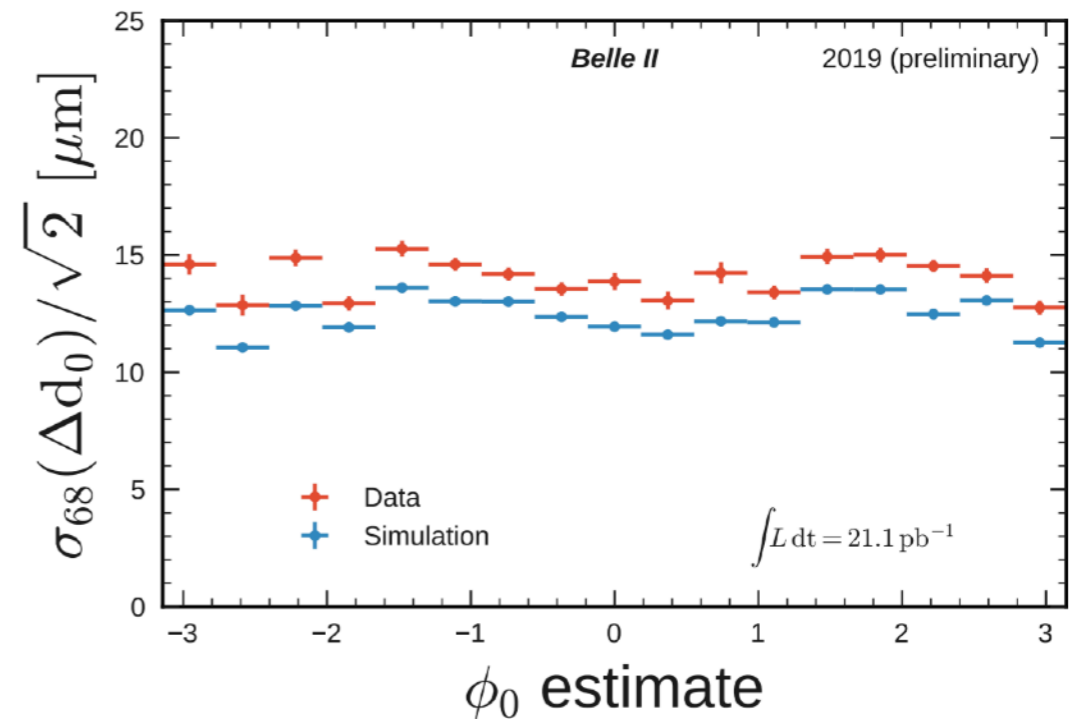
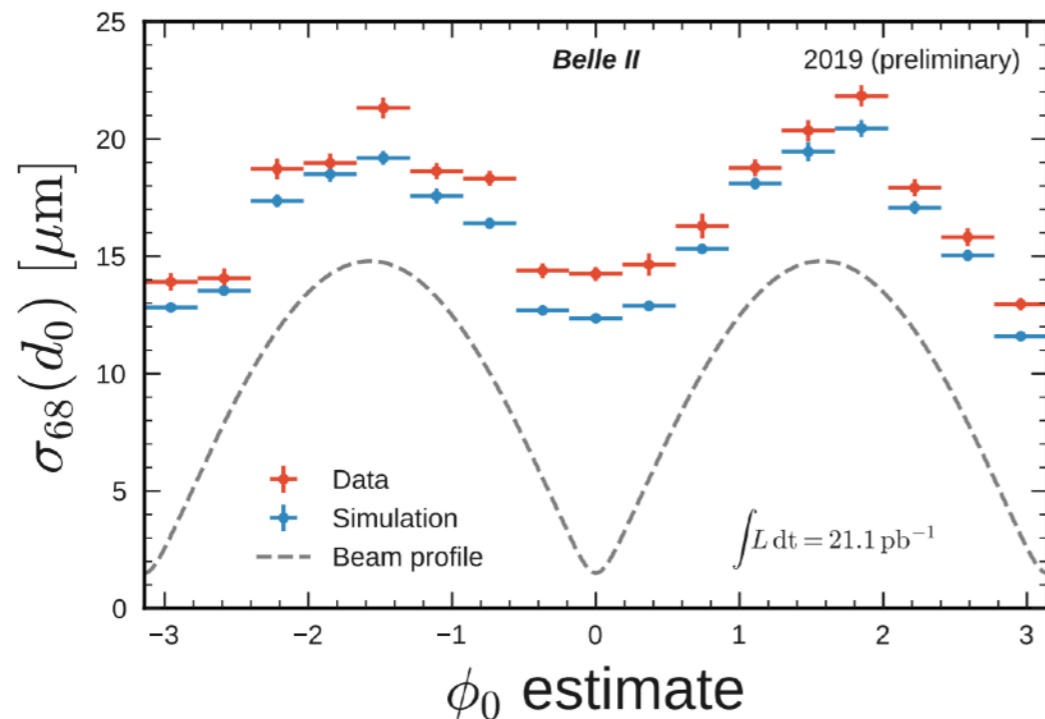
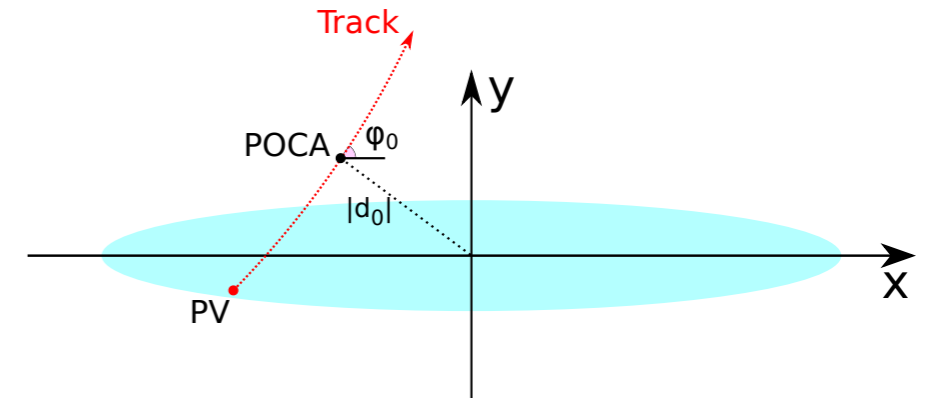
$$\sigma_{d_0} = \sqrt{\sigma_i^2 + (\sigma_x \sin \phi_0)^2 + (\sigma_y \cos \phi_0)^2}$$

- ❖ In early phase 3, $\sigma_x = 14.8\mu\text{m}$ and $\sigma_y = 1.5\mu\text{m}$

- ❖ The intrinsic resolution is estimated by

$$\Delta d_0 \equiv d_0(t_-) + d_0(t_+),$$

from 2-track (t_- and t_+) events, which are produced back-to-back.



- ❖ Good agreement observed between data and MC expectation

Summary

- ❖ The DEPFET concept combines the detection together with the in-pixel amplification by integration, on each pixel, of a FET into a fully depleted silicon bulk.
- ❖ The first real beam experience with a completely new detector type (DEPFET) and half of the full scale has been achieved.
 - ❖ Challenging operating conditions close to the IP at a very ambitious machine like SuperKEKB
- ❖ Good PXD performance is demonstrated in the 2019 spring runs.
 - ❖ Well controlled thermal performance
 - ❖ Efficiency -> further module optimisation possible
 - ❖ Impact parameter resolution very close to MC expectation